University of Copenhagen

Master's Thesis

Cavity-based quantum memory for light with inhomogeneously coupled atoms

Johann Sebastian Kollath-Bönig

supervised by

Anders Søndberg Sørensen

March 6, 2018

Acknowledgements

I would like to thank my supervisor Anders Søndberg Sørensen for introducing me to this project and always providing substantial help when needed. He guided me through this project with great insight for which I am very grateful.

Contents

Chapter 1

Introduction

Quantum mechanics allows for the creation of non-classical states with exotic behavior, for which superposition of distinct states and entanglement are the two most prominent examples. The mobility of photons and their coherence, due to weak interaction with the environment, make light the preferred carrier for the transmission of such quantum states. It is therefore of fundamental interest to study how quantum states of light can be manipulated and coupled to other physical systems. One particular area of interest is in this connection the storage of quantum light states. The most simple approach for this, storing a single photon in a single atom via absorption and then emitting a single photon, is not very effective because of the weak optical coupling of a single atom. With the development of cavity quantum electron dynamics the light-matter interactions have been somewhat improved by placing up to a few atoms in high-finesse cavities. In 1999 Lene Hau et al. [1] then showed in a seminal experiment that light effectively can be slowed down when traveling through an atomic ensemble by collective quantum interference effects. This paved the way for experiments based on atomic ensembles where light has been "frozen" and therefore a quantum memory for light has been created. Atomic ensembles consisting of many atoms can interact much more strongly with optical light and provide better storage for light via collective superposition states.

The study of quantum memories has the potential to answer some fundamental questions about the nature of quantum mechanics, such as the time duration over which quantum coherences can be maintained. Furthermore, quantum memories have promising applications within quantum information, which connects quantum mechanics with information science. In quantum information the equivalent to classical bits are qubits, which can be in one of two states or a superposition thereof. A system with X qubits can therefore be in a superposition of 2^X states and allow for the parallel processing of an enormous number of states in a quantum computer. Information encoded in qubits can also be transferred securely through public channels with quantum cryptography. In many areas of quantum information a quantum memory, which can store and release qubits on-demand, is a key component for the realization of important tasks. Because quantum error-correction can be applied to released qubits, quantum memories do not have to be completely lossless. A high efficiency is nevertheless required. At the very least, the efficiency has to be above 50 % in most quantum information applications, such that outgoing quantum states

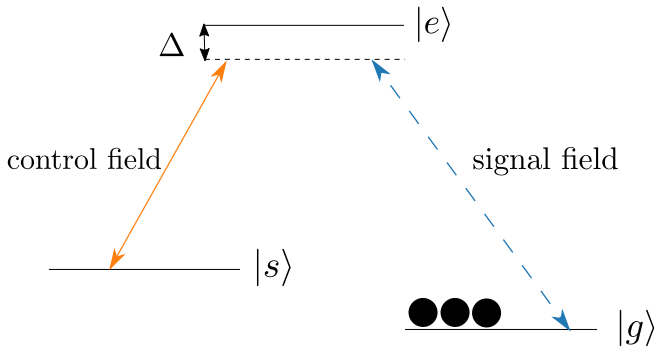

Figure 1.1: The Λ-type level structure of an optically controlled quantum memory, which allows for Raman-transitions between the ground states $|g\rangle$ and $|s\rangle$ via the excited state $|e\rangle$.

remain in the realm of the no-cloning theorem and error-correcting codes can be used.

Although a lot of progress has been made within the recent decade, it has been difficult to build efficient, scalable quantum memories with long storage times. For a long time even the most efficient quantum memories had efficiencies below the 50 % threshold [2]. Only recently has a quantum memories with μs storage time exceeded this threshold [3]. One source for losses are inhomogeneities within the ensemble with regard to the light-matter interaction. This includes inhomogeneities due to variations in the intensity of the optical light over the interaction region and inhomogeneities due to differences within the ensemble such as inhomogeneous broadening. Despite this is well-known, only one theoretical article has analyzed the effect of inhomogeneities and only with regard to inhomogeneous broadening [4]. In this thesis we will investigate further how inhomogeneities affect the storage and retrieval efficiencies for quantum memories within a cavity. Moreover, we are interested in finding the optimal storage and retrieval strategies for such systems.

In the remaining part of this chapter, a brief introduction into quantum light storage is given. It has to be mentioned that a number of excellent review articles exist on this topic [5, 6, 7].

1.1 Quantum memories

In optically controlled memories excitations are transferred to and from the atomic ensemble via a Λ-shaped energy structure as seen in Figure 1.1. A strong optical control field is necessary to initiate and maintain the interaction between the weak signal field and the atomic medium. The individual atoms have a Λ-type level structure consisting of two ground states $|g\rangle$ and $|s\rangle$ and an excited state $|e\rangle$. Transitions between the two ground states are dipole-forbidden and therefore both $|g\rangle$ and $|s\rangle$ are stable. However, by coupling the weak signal field to the $|g\rangle$ - $|e\rangle$ transition and the control field to the $|s\rangle$ - $|e\rangle$ transition, it is possible to allow for transitions between the populated ground state $|g\rangle$ and the empty ground state $|s\rangle$ via the excited state, a so-called Raman transition. Both light field are configured in such a way

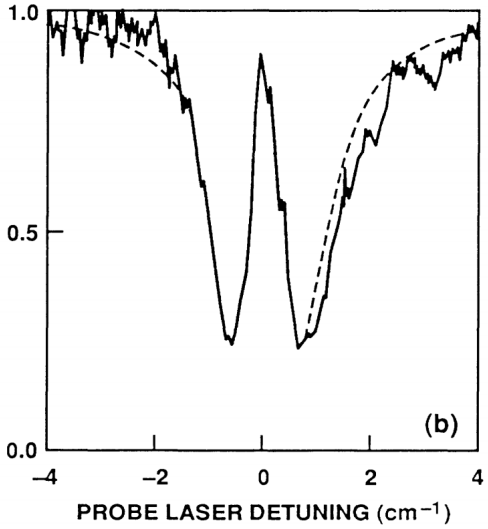

Figure 1.2: Electromagnetically induced transparency (EIT) as first observed by Boller et al. in 1991 [10]. The transmission is shown as a function of the probe laser detuning.

that they have the same detuning Δ from the excited state, which is also referred to as two-photon resonance. Under ideal conditions one optical excitation from signal field is then transferred to one collective atomic spin excitation (also called spin wave) during storage and vice versa during retrieval. The atomic excitation corresponds in this case to one spin being flipped. However, it is unknown which atomic spin in the ensemble has been flipped and a collective symmetric state is therefore created. Assuming that all N atoms initially are in the ground state $|g_1, \ldots, g_N\rangle$ the storage procedure of the single photon state $|1\rangle$ corresponds to

$$|1\rangle |g_1, \ldots, g_N\rangle \rightarrow |0\rangle \sum_{i=1}^{N} \frac{1}{\sqrt{N}} e^{i\omega_{gs} z_i/c} |g_1, \ldots, s_i, \ldots, g_N\rangle \tag{1.1}$$

where ω_{gs} is the difference in frequency of the signal and control fields, z_i the position of the j'th atom and c the speed of light [8]. Both electromagnetically induced transparency (EIT) and Raman-based protocols make use of optically controlled memories. In fact, it has been shown in [9] that they for theoretical considerations can be thought of special cases of a more general limit, where the excited state $|e\rangle$ can be adiabatically eliminated.

Protocols based on EIT use configurations with small detuning Δ compared to the linewidth of the excited state. In this regime the atomic medium becomes transparent with respect to a narrow range of frequencies, i.e., the signal field is not absorbed by the atomic ensemble and travels through the medium, if it fits into the transparency window, see Figure 1.2. This effect is based on destructive quantum interference between the control and signal fields and referred to as electromagnetically induced transparency (EIT) [11, 12, 7]. Because of the narrow transparency window the refractive index varies sharply with frequency close to resonance. A wave packet is therefore propagating through the medium with a reduced group velocity.

Lowering the intensity of the control beam does then decrease the group velocity even further, such that the light pulse eventually is trapped inside the medium when the control field is turned off completely. As the group velocity decreases, the transparency window becomes also more narrow. The wave packet is however spatially compressed at the same rate, such that it always fits inside the transparency window if it does so initially. Furthermore the spatial compression ensures that the pulse fits into the atomic medium.

Technically speaking it is wrong to suggest that the group velocity of the pulse becomes zero and the pulse therefore is "frozen" inside the ensemble. The quantum state of the complete system is described by a so-called dark-state polariton [8, 13]. As the signal field enters the medium, it also creates atomic coherences in the $|g\rangle$ - $|s\rangle$ transition. When the control field has been switched off gradually, the shape of the signal field has been transferred to low-energy atomic coherences and no optical field is present [11]. Most of the energy and momentum has previously been transferred into the control beam. Under ideal conditions the atomic coherences are independent of the excited state and therefore called "dark". This eliminates spontaneous emission from the excited state as a source for loss. Turning the control field back on reverses the process, such that the shape of the atomic coherences is transferred back to a quantum field with energy applied through the control field.

In protocols which use the Raman configuration, the two pulses have detunings far-off resonance such that the detuning is much larger than the linewidth of the excited state. For far-off resonant Raman transitions the excited state can be eliminated and the three-level system is effectively reduced to a two-level system involving only the ground states [14, 15, 16]. Again this reduces the sensitivity to spontaneous emission of the excited state. Because the Raman condition can be fulfilled for a wide range of frequencies, high-bandwidth storage of light is possible.

An alternative to optically controlled memories are memories based on the photon echo technique. They rely on the inhomogeneous broadening of the medium, which arises when the individual atoms in the ensemble have different detunings Δ_i with respect to the same optical field. A disadvantage of optically controlled memories is that they are inefficient for the storage of multi-mode signals, whereas the inhomogeneous broadening in photon-echo memories makes them intrinsically multi-mode [6]. The most simple protocol based on photon echo absorbs the signal field using a two-level system without a control pulse. Because of the inhomogeneous broadening the atoms, which have absorbed a photon, precess at different frequencies. The storage procedure of a single photon corresponds therefore to [17]

$$|1\rangle |g_1, \ldots, g_N\rangle \rightarrow |0\rangle \sum_{i=1}^{N} \frac{1}{\sqrt{N}} e^{i\Delta_i t} e^{i\omega z_i/c} |g_1, \ldots, e_i, \ldots, g_N\rangle \tag{1.2}$$

where ω is the frequency of the signal field. These unaligned precession frequencies prevent the ensemble from emitting optical excitations, because the atoms interfere destructively. After some time T the atoms have accumulated a phase $e^{i\Delta_i T}$ and a pulse is applied, which reverses the detunings such that $\Delta_i \rightarrow -\Delta_i$. Subsequently at time $2T$ the individual atoms have attained an additional phase $e^{-i\Delta_i T}$, which cancels the previously accumulated phase between absorption and the application of the pulse at time T. The polarizations of all atoms will therefore be equal, leading

to the emission of the stored signal field at time $2T$ [7, 5]. To allow for longer storage times and make the process truly on-demand a third intermediate level can be added to the structure. After absorption of the signal field, a pulse transfers the excited state population to the intermediate state, where the atomic precession effectively is stopped. A second pulse can then be applied to initiate retrieval of the signal field by returning the population to the excited state and reversing detuning, which then, as before, leads to emission when the phases are aligned [6].

Generally the more efficient protocols for photon echo memories can be classified as based on controlled reversible inhomogeneous broadening (CRIB) [18] or atmoic frequency comb (AFC) protocols [17]. They differ in the initial distribution of detunings Δ_i, which for AFC is described by a periodic comb-like structure.

1.2 Implementations

Some of the most important early developments in the realization of quantum memories have been achieved with memories based on alkali metal vapour isotopes, since they offer easily accessible optical transitions near infrared range at both cold and hot temperatures. The first successful implementations of an EIT-memory for classical light in 2001 have been based on hot rubidium vapour cells and magnetically trapped, cold cloud of sodium atoms with storage times of 0.2 ms and 0.9 ms [19, 20]. Storage of quantum light was demonstrated in 2004 with caesium vapour [21]. In more recent experiments the storage times lie typically around 100 μs for hot gases and around 1 s for cold gases confined in magneto-optical traps. With the additional use of optical lattices it was possible to extend storage times to 16 s in 2013 [22]. A main disadvantage of alkali vapour is the loss introduced by the motion of the atoms which destroys coherences and removes atoms from the interaction area. Cooling to μK temperatures in optical traps helps to increase the performance of alkali vapour based quantum memories. Still, the resulting efficiencies and storage times make it very challenging to realize practical tasks such as long-distance communication.

Quantum memories based on rare-earth-ion-doped crystals are more promising candidates for practical applications, because they do not suffer from atomic diffusion and have a large optical density. This leads to better scalability and longer storage times at cryogenic temperatures. In [23] a storage time of up to 1 min has been achieved for classical light by applying the EIT storage protocol in Pr^{3+} ion doped Y_2SiO_5 crystals ($Pr^{3+} : Y_2SiO_5$) with an efficiency of 0.4 %. Ground-state coherences in $Eu^{3+} : Y_2SiO_5$ of six hours have been demonstrated in [24], but without using the medium as a quantum memory. Solid state systems are affected by intrinsic inhomogeneities such as inhomogeneous broadening. This can lead to losses in EIT and Raman-based protocols, which are based on homogeneous optical transitions. However, they are a useful resource in the application of CRIB and AFC protocols. The multimode capacity of these protocols has been demonstrated in [25] and [17]. The efficiency can often be improved by placing the light-matter interface inside an optical cavity, because it increases the optical depth. For rare-earth-ion-doped crystal cavity enhancement has been demonstrated in [26].

Nitrogen vacancy centres in diamond have a stronger light coupling compared to

rare-earth-ion-doped crystals and might therefore be better suited for large-scale fabricational processes and optical on-chip implementation on nanometer scale. Parts of the EIT-protocol and spin coherences have been demonstrated, but without implementing a quantum memory [27]. Experiments for demonstrating optical storage have until now only been proposed. Apart from the described implementations there are also efforts to realize quantum light storage with molecules [28] and phononic modes in pure diamond [29].

1.3 Applications

One of the most promising applications for quantum memories is the realization of long-distance quantum communication. Photons losses prevent the transmission of quantum information via optical fibers to be feasible for longer distances. These photon losses can be overcome by the application of quantum repeaters, which rely on the entanglement of multiple quantum memories. Quantum repeaters divide the quantum channel into multiple segments, where each end node consists of a quantum memories and is entangled with the other end node in the segment. Afterwards entanglement is created between neighboring segments through entanglement swapping. Repeating this process several times can then lead to entanglement between the two end nodes of the entire quantum channel. Once entanglement has been established over this long distance, quantum teleportation can be used to send the quantum information to the other end without being affected by photon losses. Quantum memories are necessary components of quantum repeaters, which have to overcome photon losses, because several attempts may be needed to create entanglement within one segment. The entanglement can be created by detecting a photon in the middle of the segment, which has been emitted from one of the end nodes and does not contain information about its path. As soon as a photon has been detected in one segment, the entanglement has to be stored until entanglement has been created in the neighboring segment and entanglement swapping can be performed. Many experiments for quantum repeaters have implemented the so-called DLCZ protocol, which is based on these steps and uses off-resonant Raman quantum memories [30]. More efficient and complicated protocols are presented in [31, 32]. Other important applications for quantum memories include the realization of single-photon detectors and components essential for linear-optical quantum computation [33].

Chapter 2

Light-matter interaction

In this chapter we will write down the equations of motions for a Λ-type quantum memory with inhomogeneities in a cavity and define the storage and retrieval efficiencies, which can be used to asses the performance of a quantum memory.

We will describe the system with a Λ-type level structure consisting of two ground states $|g\rangle$ and $|s\rangle$ and an excited state $|e_1\rangle$. Furthermore, we allow the ground states to couple to several additional excited states $|e_j\rangle$ as seen in Figure 2.1. This is especially relevant for quantum memories based on NV-centers, where closely spaced excited states have been observed to affect the performance [27]. The weak signal field couples to the $|g\rangle$ - $|e_j\rangle$ transitions with single-atom coupling constants $g_j^{(i)}$ and a classical control field is used to couple the $|s\rangle$ - $|e_j\rangle$ transitions with single-atom Rabi oscillations $\Omega_j^{(i)}$. Both light field are configured in such a way that they are in two-photon resonance with single-atom detunings $\Delta_j^{(i)}$ from the excited states. By using single-atom parameters, we can account for inhomogeneities in the quantum memory. The atomic ensemble is placed within a cavity in order to increase the optical depth and therefore the coherent coupling between the incoming light and the atoms. As we will find out, the cavity model only allows for storage in one specific spin-wave mode for homogeneous Rabi oscillations and detunings. This is in contrast to the free-space model, where the incoming light can be coupled to different spin-wave modes. With inhomogeneous Rabi oscillations and detunings included, several spin-wave modes will however also become available in the cavity model. The system has for the homogeneous case with one excited level state been studied in detail by Gorshkov et al. [9].

2.1 The Hamiltonian

First we define the electric-fields in order to find the full Hamiltonian of the system. In our model we assume that the light fields are propagating along the z-axis. The signal field inside the cavity is described by the vector operator

$$\hat{\mathbf{E}}_1(z) = \boldsymbol{\epsilon}_1 \left(\frac{\hbar\omega_1}{2\epsilon_0 V} \right)^{1/2} \left(\hat{\mathcal{E}} e^{i\omega_1 z/c} + \hat{\mathcal{E}}^\dagger e^{-i\omega_1 z/c} \right) \tag{2.1}$$

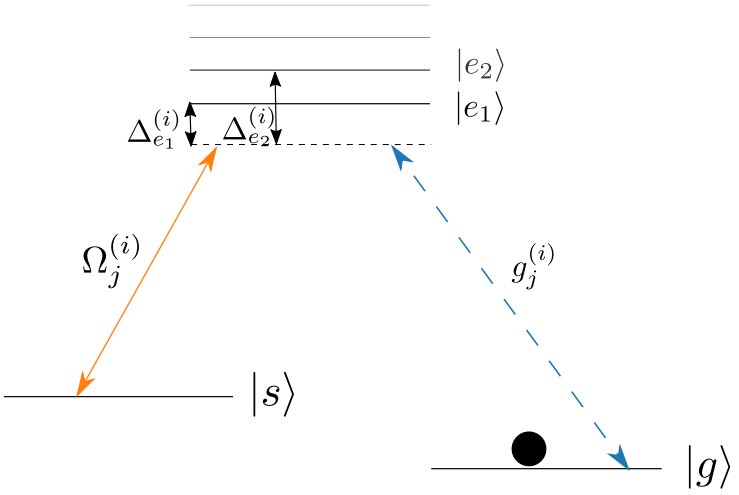

Figure 2.1: The level structure of an optically controlled quantum memory with several excited states.

where $\hat{\mathcal{E}}$ is the mode annihilation operator, ω_1 is the mode frequency, $\boldsymbol{\epsilon}_1$ is the polarization unit vector, ϵ_0 is the permittivity of free space, V is the quantization volume for the field and c is the speed of light.

The classical control field with frequency ω_2, polarization unit vector $\boldsymbol{\epsilon}_2$ and amplitude $\mathcal{E}_2(t)$ is described by the electric-field vector

$$\mathbf{E}_2(z,t) = \boldsymbol{\epsilon}_2 \mathcal{E}_2(t) \cos\left[\omega_2 \left(t - z/c\right)\right]. \tag{2.2}$$

Because the Hilbert space of the system in the cavity can be decomposed into the Hilbert spaces for all the single atoms and the electromagnetic field, the ground state Hamiltonian consists of the sum of Hamiltonians for the individual atoms and the signal field.

$$\hat{H}_0 = \hbar\omega_1 \hat{\mathcal{E}}^\dagger \hat{\mathcal{E}} + \sum_{i=1}^{N} \left(\hbar\omega_g^{(i)} \hat{\sigma}_{gg}^{(i)} + \hbar\omega_s^{(i)} \hat{\sigma}_{ss}^{(i)} + \sum_{j=e_1 \ldots e_N} \hbar\omega_j^{(i)} \hat{\sigma}_{jj}^{(i)} \right) \tag{2.3}$$

Here $\hat{\sigma}_{\mu\nu}^{(i)} = |\mu\rangle_{i\,i}\langle\nu|$ is the internal state operator of the ith atom between states $|\mu\rangle$ and $|\nu\rangle$. We make use of the electric dipole approximation when defining the interaction part of the Hamiltonian. In this approximation we assume the electrical field to be spatially uniform. This is valid for optical frequencies with wavelength λ, because $\lambda \gg r_0$ where r_0 is the bohr radius. Furthermore, we only have to keep the dominant term in a multipole expansion. All terms other than the dipole term are negligible in this case. In the presence of an electrical field $\hat{\mathbf{E}}$ where the atom develops an electric dipole moment $\hat{\mathbf{d}}$ the interaction Hamiltonian is then $\hat{H}_{\text{int}} = -\hat{\mathbf{d}} \cdot \hat{\mathbf{E}}$. This

translates in our model to:

$$\begin{aligned}\hat{H}_{\text{int}} &= -\sum_{i=1}^{N} \hat{\mathbf{d}}_i \cdot \left[\mathbf{E}_2\left(z_i,t\right) + \hat{\mathbf{E}}_1\left(z_i\right)\right] \\ &= -\hbar \sum_{i=1}^{N} \sum_{j=e_1 \ldots e_N} \Big[\Omega_j^{(i)}(t)\hat{\sigma}_{js}^{(i)}\left(e^{i\omega_2(t-z_i/c)} + e^{-i\omega_2(t-z_i/c)}\right) \\ &\qquad + g_j^{(i)}\hat{\sigma}_{jg}^{(i)}\left(\hat{\mathcal{E}}e^{i\omega_1 z_i/c} + \hat{\mathcal{E}}^{\dagger}e^{-i\omega_1 z_i/c}\right)\Big] + \text{H.c.} \end{aligned} \tag{2.4}$$

Here we have made use of the fact that the transition between the ground states is dipole forbidden and therefore $\langle e|\left(\hat{\mathbf{d}}_i \cdot \boldsymbol{\epsilon}_{1,2}\right)|s\rangle = \langle s|\left(\hat{\mathbf{d}}_i \cdot \boldsymbol{\epsilon}_{1,2}\right)|e\rangle = 0$. Furthermore we have assumed that the signal field only couples to the $|g\rangle$ - $|e_j\rangle$ transitions and the control field only to the $|s\rangle$ - $|e_j\rangle$ transitions. In experiment this can be established by using left-hand and right-hand polarized light. Therefore, we only had to introduce the Rabi frequency of the classical field and the coupling constant between the atoms and the signal field in the previous equation.

$$\Omega(t)_j^{(i)} = {}_i\langle e_j|(\hat{\mathbf{d}}_i \cdot \boldsymbol{\epsilon}_2)\,|s\rangle_i \,\frac{\mathcal{E}_2(t)}{2\hbar} \qquad g_j^{(i)} = {}_i\langle e_j|(\hat{\mathbf{d}}_i \cdot \boldsymbol{\epsilon}_1)\,|g\rangle_i \sqrt{\frac{\omega_1}{2\hbar\epsilon_0 V}} \tag{2.5}$$

The full Hamiltonian can be further simplified by going into a different frame of reference where a unitary transformation is applied such that the transformed Hamiltonian is $\hat{\tilde{H}} = i\hbar\dot{\hat{U}}^{\dagger}\hat{U} + \hat{U}^{\dagger}\hat{H}\hat{U}$. In our case we do this by applying the unitary transformation

$$\hat{U} = \exp\left\{-it\sum_i \left[\omega_g^{(i)}\hat{\sigma}_{gg}^{(i)} + \omega_s^{(i)}\hat{\sigma}_{ss}^{(i)} + \sum_j \left(\omega_j^{(i)} - \Delta_j^{(i)}/\hbar\right)\hat{\sigma}_{jj}^{(i)}\right]\right\}. \tag{2.6}$$

When applying the transformation $\hat{U}^{\dagger}\hat{H}\hat{U}$ to the interaction part of the Hamiltonian we get terms with the form

$$\Omega_j^{(i)}(t)\hat{\sigma}_{js}^{(i)}\left(e^{i\omega_2(2t-z_i/c)} + e^{i\omega_2 z_i/c}\right) + g_j^{(i)}\hat{\sigma}_{jg}^{(i)}\left(\hat{\mathcal{E}}e^{i\omega_1 z_i/c} + \hat{\mathcal{E}}^{\dagger}e^{i\omega_1(2t-z_i/c)}\right) + \text{H.c.}$$

In the so-called rotating wave approximation the terms with $e^{\pm 2i\omega_{1,2}t}$ are neglected. Compared to the time of the optical-atomic interaction, those terms with the optical frequency are varying very quickly and therefore average to zero. Furthermore we redefine $\hat{\tilde{\sigma}}_{js}^{(i)} = \hat{\sigma}_{js}^{(i)}e^{i\omega_2 z_i/c}$, $\hat{\tilde{\sigma}}_{jg}^{(i)} = \hat{\sigma}_{jg}^{(i)}e^{i\omega_1 z_i/c}$ and remove the tilde in the notation from now on. Applying the full transformation for each atom gives then the effective rotating frame Hamiltonian

$$\hat{\tilde{H}}^{(i)} = \sum_{j=e_1 \ldots e_N} \left[\hbar\Delta_j^{(i)}\hat{\sigma}_{jj}^{(i)} - \left(\hbar\Omega_j^{(i)}(t)\hat{\sigma}_{js}^{(i)} + \hbar\hat{\mathcal{E}}g_j^{(i)}\hat{\sigma}_{jg}^{(i)} + \text{H.c.}\right)\right]. \tag{2.7}$$

The detuning with respect to the excited levels of each atom is here defined as $\Delta_j^{(i)} = \hbar\omega_j^{(i)} - \hbar\omega_g^{(i)} - \hbar\omega_1 = \hbar\omega_j^{(i)} - \hbar\omega_s^{(i)} - \hbar\omega_2$. We therefore allow the model to incorporate inhomogenoeus broadening. However, we neglect the difference in detuning between the two optical transitions such that each atom is at two-photon resonance. This is accurate if the two ground states are degenerate.

2.2 Dynamics

In our model excitations from the incoming signal field $\hat{\mathcal{E}}_{\text{in}}$ are transferred to the spin wave mode, which is created through atomic transitions represented by the atomic operator $\hat{\sigma}_{gs}^{(i)}$. During retrieval the spin-wave is then retrieved onto the outgoing quantum field $\hat{\mathcal{E}}_{\text{out}}$. We are therefore especially interested in the dynamics of those operators and their relation.

The input-output relation of the qauntum field in the cavity with a cavity decay rate of 2κ is [34]

$$\hat{\mathcal{E}}_{\text{out}}(t) = \sqrt{2\kappa}\hat{\mathcal{E}}(t) - \hat{\mathcal{E}}_{\text{in}}(t). \tag{2.8}$$

We know that the commutation relations between the atomic operators are $[\hat{\sigma}_{\mu\nu}^{(i)}, \hat{\sigma}_{\alpha\beta}^{(j)}] = \delta_{ij}(\delta_{\nu\alpha}\hat{\sigma}_{\mu\beta}^{(i)} - \delta_{\mu\beta}\hat{\sigma}_{\alpha\nu}^{(i)})$. This allows us to use Heisenberg's equation of motion. We also include decay for the atomic operators, which then requires the introduction of Langevin noise operators $\hat{F}_{\mu\nu}$.

$$\begin{aligned}
\dot{\hat{\mathcal{E}}} =& -\kappa\hat{\mathcal{E}} + i\sum_{i=1}^{N}\sum_{j=e_1\ldots e_N} g_j^{(i)}\hat{\sigma}_{gj}^{(i)} + \sqrt{2\kappa}\hat{\mathcal{E}}_{\text{in}} \\
\dot{\hat{\sigma}}_{gj}^{(i)} =& -\left(\gamma + i\Delta_j^{(i)}\right)\hat{\sigma}_{gj}^{(i)} + i\Omega_j^{(i)}\hat{\sigma}_{gs}^{(i)} + ig_j^{(i)}\hat{\mathcal{E}}\left(\hat{\sigma}_{gg}^{(i)} - \hat{\sigma}_{jj}^{(i)}\right) + \hat{F}_{gj}^{(i)} \\
\dot{\hat{\sigma}}_{gs}^{(i)} =& -\gamma_s + i\sum_{j=e_1\ldots e_N}\Omega_j^{*(i)}\hat{\sigma}_{gj}^{(i)} - i\hat{\mathcal{E}}\sum_{j=e_1\ldots e_N} g_j^{(i)}\hat{\sigma}_{js}^{(i)} + \hat{F}_{gs}^{(i)}
\end{aligned} \tag{2.9}$$

Here we have introduced the decay rate γ of the optical coherences $\hat{\sigma}_{gj}$. Both dephasing and radiative decay of the excited state γ_e can be included in the decay rate γ such that $\gamma = \gamma_e/2 + \gamma_{\text{deph}}$. However, we will neglect the slow decay of the spin wave and set $\gamma_s = 0$. A nonzero decay γ_s would simply introduce an exponential decay [9]. Furthermore, in [35] it has been found that the spin wave decay can lead to a decrease in efficiency for large optical depth. Another assumption we will make is that all atoms are in the ground state $|g\rangle$ at all times and therefore assume $\hat{\sigma}_{gg}^{(i)} \approx 1$ and $\hat{\sigma}_{ss}^{(i)} \approx \hat{\sigma}_{ee}^{(i)} \approx \hat{\sigma}_{es}^{(i)} \approx 0$. This simple reason for this is that we have a very large number of atoms and most of them will remain in the ground state during the interaction. It also follows from this assumption that all normally ordered noise correlations are zero, meaning that the incoming noise is vacuum and that the noise operators have no effect on the dynamics. Furthermore, having a cavity in the "bad cavity" limit where $\kappa \gg g^{(i)}\sqrt{N}$ allows us to adiabatically eliminate $\hat{\mathcal{E}}$. Using all of those assumptions do then simplify the equations of motions to give

$$\begin{aligned}
\hat{\mathcal{E}}_{\text{out}} =& \hat{\mathcal{E}}_{\text{in}} + i\sqrt{\frac{2}{\kappa}}\sum_{i=1}^{N}\sum_{j=e_1\ldots e_N} g_j^{(i)}\hat{\sigma}_{gj}^{(i)} \\
\dot{\hat{\sigma}}_{gj}^{(i)} =& -\left(\gamma + i\Delta_j^{(i)}\right)\hat{\sigma}_{gj}^{(i)} - \frac{g_j^{(i)}}{\kappa}\sum_{k=1}^{N}\sum_{l=e_1\ldots e_N} g_l^{(k)}\hat{\sigma}_{gl}^{(k)} + i\Omega_j^{(i)}\hat{\sigma}_{gs}^{(i)} + i\sqrt{\frac{2}{\kappa}}g_j^{(i)}\hat{\mathcal{E}}_{\text{in}} \\
\dot{\hat{\sigma}}_{gs}^{(i)} =& i\sum_{j=e_1\ldots e_N}\Omega_j^{*(i)}\hat{\sigma}_{gj}^{(i)}.
\end{aligned} \tag{2.10}$$

We can now find the relation between the incoming light and the spin wave for the storage process and the relation between the spin wave and the outgoing light for the retrieval process.

2.3 Process efficiency

Because we have introduced decay in our model, the retrieved state is not going to be identical to the incoming state. In order to asses the performance of the quantum memory it is therefore essential to find a figure of merit. All of the mappings we consider can be characterized by the efficiency η, which is defined as the probability to find a given initial excitation in the output mode after the interaction. In order to quantify the number of stored excitations in the atomic system, we define the annihilation operator for the collective spin-wave mode $\hat{s}$ fulfilling the commutation relation $[\hat{s}(t), \hat{s}^\dagger(t)] = 1$, which for the symmetric spin-wave mode would have the form $\hat{s} = \sum_i \hat{\sigma}_{gs}^{(i)}/\sqrt{N}$. The storage efficiency is then given by

$$\eta_s = \frac{\text{(number of stored excitations)}}{\text{(number of incoming photons)}} = \frac{\left\langle \hat{s}^\dagger(T)\hat{s}(T) \right\rangle}{\int_0^T dt \left\langle \hat{\mathcal{E}}_{\text{in}}^\dagger(t)\hat{\mathcal{E}}_{\text{in}}^\dagger(t) \right\rangle}. \tag{2.11}$$

Here the spin-wave operator $\hat{s}(T)$ is only going to depend on a linear combination of $\hat{\mathcal{E}}_{\text{in}}$, $\hat{s}(0)$ and $\{\hat{\sigma}_{gj}^{(i)}(0)\}$, because we in our model assume that the incoming noise is vacuum. No excitations are present in the initial state, so $\hat{s}(0)$ and $\{\hat{\sigma}_{gj}^{(i)}(0)\}$ give zero when applied to this state. Furthermore assuming that the signal field only has excitations in one mode with annihilation operator $\hat{a}_0$ and envelope shape $h_0(t)$ nonzero on $[0, T]$ such that $\hat{\mathcal{E}}_{\text{in}} = h_0(t)\hat{a}_0$, we can treat the equations of motions as complex number equations, if we only are interested in finding efficiencies. From now on we are going to do this.

Compared to calculating the storage efficiency it is however more convenient to calculate the efficiency of the retrieval process. For the purpose of calculating the retrieval efficiency, we can similarly use the complex number representation, because $\hat{\mathcal{E}}_{\text{out}}$ only is going to depend on $\hat{s}(T_r)$ when applied to the initial state. The retrieval efficiency is in the complex number representation defined as follows

$$\eta_r = \frac{\text{(number of retrieved photons)}}{\text{(number of stored excitations)}} = \int_{T_r}^{\infty} dt |\mathcal{E}_{\text{out}}(t)|^2 \tag{2.12}$$

for the initial condition $|s(T_r)|^2 = 1$. Instead of having to find the sum over N functions when calculating the storage efficiency, we here have an integral over a single function.

It can therefore be very useful to apply the so-called time-reversal argument, which allows us to focus the analysis on the retrieval process. According to the time-reversal argument, the efficiency for storing the time reverse of the output field $\mathcal{E}_{\text{in}}(t) = \mathcal{E}_{\text{out}}^*(T_{\text{out}} - t)$, with $\Omega^*(T_{\text{out}} - t)$, the time reverse of the retrieval control filed, into the spin wave $s^*(T)$ is equal to the retrieval efficiency from $s(T)$. However, we have to make sure that we store into the spin-wave mode we also later want to retrieve from. But more on this in chapter 5, where storage followed by retrieval is analyzed.

2.4 Inhomogenous coupling constant $g^{(i)}$

In this section we are going to find an analytical solution of the retrieval efficiency for an ensemble of atoms with different coupling constants $g^{(i)}$ but identical Rabi oscillation Ω. Furthermore we are going to consider a Λ energy level scheme with only one excited level and without inhomogeneous broadening (same detuning Δ for all atoms). During the retrieval process there is no incoming quantum field $\hat{\mathcal{E}}_{in} = 0$, the equations of motion are therefore as follows:

$$\begin{aligned}
\mathcal{E}_{\text{out}} =& i\sqrt{\frac{2}{\kappa}}\sum_{i=1}^{N} g^{(i)}\sigma_{\text{ge}}^{(i)} \\
\dot{\sigma}_{ge}^{(i)} =& -\left(\gamma + i\Delta\right)\sigma_{ge}^{(i)} - \frac{g^{(i)}}{\kappa}\sum_{j=1}^{N} g^{(j)}\sigma_{ge}^{(j)} + i\Omega\sigma_{gs}^{(i)} \\
\dot{\sigma}_{gs}^{(i)} =& i\Omega^{*}\sigma_{ge}^{(i)}
\end{aligned} \tag{2.13}$$

The structure of the set of equations allows us to reduce the number of equations by introducing two new collective variables.

$$p = \frac{\sum_i g^{(i)}\sigma_{ge}^{(i)}}{\sqrt{\sum_i \left|g^{(i)}\right|^2}} \qquad s = \frac{\sum_i g^{(i)}\sigma_{gs}^{(i)}}{\sqrt{\sum_i \left|g^{(i)}\right|^2}} \tag{2.14}$$

In operator representation they would act as annihilation operators and fulfill the commutation relation $[\hat{s}, \hat{s}^{\dagger}] = 1$ and $[\hat{p}, \hat{p}^{\dagger}] = 1$. Because we can describe the spin wave s with this single collective variable, only this specific collective mode is accessible. For homogeneous $g^{(i)}$ it would therefore only be possible to couple to the symmetric mode ($s = \sum_i \sigma_{gs}^{(i)}/\sqrt{N}$ for real g), where all excitations are distributed evenly among the atoms. But also for inhomogeneous $g^{(i)}$ it is only possible to couple to the mode in Eq. (2.14). The differential equations can then with the introduction of these new variables be reduced to the more simple set of equations:

$$\begin{aligned}
\mathcal{E}_{\text{out}} =& i\sqrt{2\gamma\tilde{C}}p \\
\dot{p} =& -\left[\gamma\left(1+\tilde{C}\right) + i\Delta\right]p + i\Omega s \\
\dot{s} =& i\Omega^{*}p
\end{aligned} \tag{2.15}$$

Here we also have defined the cooperativity parameter $\tilde{C} = \sum_i {g^{(i)}}^2/(\kappa\gamma)$. This shows the collective enhancement, which can be archived by using a large ensemble. A large number of atoms N increases the effective coupling constant ($\sqrt{N}g$ for homogeneous $g^{(i)}$), while not leading to any additional decay γ due to dephasing and spontaneous emission. From the set of equations we can then derive the relation $d/dt(|p|^2 + |s|^2) = -2\gamma(1+\tilde{C})|p|^2$ and finally get a result for the retrieval efficiency

$$\eta_r = \frac{\tilde{C}}{1+\tilde{C}}\left[|s(T_r)|^2 + |p(T_r)|^2 - |s(\infty)|^2 - |p(\infty)|^2\right] \tag{2.16}$$

which is reduced to $\eta_r = \tilde{C}/(1+\tilde{C})$ for the boundary conditions $|s(T_r)|^2 = 1$ and $p(T_r) = p(\infty) = s(\infty) = 0$. This result shows that the retrieval efficiency is

independent of both the detuning Δ and the shape of the control beam Ω. Moreover, inhomogeneities in the distribution of the coupling constant $g^{(i)}$ do not lead to any additional decoherence, since $\tilde{C}$ is a simple sum over the values for each atom. As we will see in the next chapters, this is not the case for inhomogeneities in $\{\Omega^{(i)}\}$ or $\{\Delta^{(i)}\}$.

Chapter 3

Model with inhomogeneities

We will now introduce two more general ways to calculate the retrieval efficiency, where we can account for inhomogeneities in the system. First, we present a simple approach to calculating the efficiency numerically for all various distributions of $\{g^{(i)}\}$, $\{\Omega^{(i)}\}$ and $\{\Delta^{(i)}\}$. The second approach will allow us to derive a symbolic expression for the efficiency if the distributions $\{g^{(i)}\}$, $\{\Omega^{(i)}\}$ and $\{\Delta^{(i)}\}$ have well-defined moments. In both cases we have to find a solution to the full set of equations of motion in Eq. (2.10), which treated as complex number equations in matrix form can be written as:

$$\begin{aligned}\mathcal{E}_{\text{out}} &= \mathcal{E}_{\text{in}} + i\sqrt{\frac{2}{\kappa}}\mathbf{g}^T\mathbf{p} \\ \dot{\mathbf{p}} &= -\mathbf{\Gamma}\mathbf{p} + \mathbf{\Omega}\mathbf{s} + i\sqrt{\frac{2}{\kappa}}\mathcal{E}_{\text{in}}\mathbf{g} \\ \dot{\mathbf{s}} &= -\mathbf{\Omega}^*\mathbf{p}\end{aligned} \tag{3.1}$$

Here, we have defined the vectors and matrices such that they include the elements for all N atoms and transitions between all ground states and excited states.

$$\begin{aligned}\mathbf{s}^T &= \begin{pmatrix}\sigma_{ge_1}^{(1)} & \dots & \sigma_{ge_1}^{(N)} & \sigma_{ge_2}^{(1)} & \dots & \sigma_{ge_2}^{(N)} & \dots & \sigma_{ge_N}^{(1)} & \dots & \sigma_{ge_N}^{(N)}\end{pmatrix} \\ \mathbf{g}^T &= \begin{pmatrix}g_{e_1}^{(1)} & \dots & g_{e_1}^{(N)} & g_{e_2}^{(1)} & \dots & g_{e_2}^{(N)} & \dots & g_{e_N}^{(1)} & \dots & g_{e_N}^{(N)}\end{pmatrix} \\ \mathbf{\Omega} &= \text{diag}\begin{pmatrix}\Omega_{e_1}^{(1)} & \dots & \Omega_{e_1}^{(N)} & \Omega_{e_2}^{(1)} & \dots & \Omega_{e_2}^{(N)} & \dots & \Omega_{e_N}^{(1)} & \dots & \Omega_{e_N}^{(N)}\end{pmatrix} \\ \mathbf{\Delta} &= \text{diag}\begin{pmatrix}\Delta_{e_1}^{(1)} & \dots & \Delta_{e_1}^{(N)} & \Delta_{e_2}^{(1)} & \dots & \Delta_{e_2}^{(N)} & \dots & \Delta_{e_N}^{(1)} & \dots & \Delta_{e_N}^{(N)}\end{pmatrix} \\ \mathbf{\Gamma} &= \tilde{\mathbf{\Delta}} + \frac{1}{\kappa}\mathbf{g}\mathbf{g}^T \qquad \tilde{\mathbf{\Delta}} = \gamma\mathbf{I} + i\mathbf{\Delta}\end{aligned} \tag{3.2}$$

Let us now take a look at the retrieval process, where there is no incoming light $\mathcal{E}_{\text{in}} = 0$. In order to determine the relation between the spin wave and the outgoing light, the differential equations become sufficiently simple when the polarization $\mathbf{p}$ is adiabatically eliminated, where we assume $\dot{\mathbf{p}} = 0$. This approximation is valid for a smooth input pulse with a sufficiently long duration and a smooth and sufficiently

weak retrieval control pulse [9]. This simplifies the system to

$$\begin{aligned} \mathcal{E}_{\text{out}} =& \mathbf{v}^\dagger \mathbf{s} \\ \dot{\mathbf{s}} =& -\mathbf{A}\mathbf{s} \end{aligned} \tag{3.3}$$

where we have defined

$$\mathbf{v}^\dagger = -\sqrt{\frac{2}{\kappa}}\mathbf{g}^T\mathbf{\Gamma}^{-1}\mathbf{\Omega} \quad \text{and} \quad \mathbf{A} = \mathbf{\Omega}^*\mathbf{\Gamma}^{-1}\mathbf{\Omega}. \tag{3.4}$$

The so-called Sherman-Morrison formula can be used to find the inverse of the matrix $\mathbf{\Gamma}$.

$$\mathbf{\Gamma}^{-1} = \tilde{\mathbf{\Delta}}^{-1} - \frac{\tilde{\mathbf{\Delta}}^{-1}\mathbf{g}\mathbf{g}^T\tilde{\mathbf{\Delta}}^{-1}}{\kappa + \mathbf{g}^T\tilde{\mathbf{\Delta}}^{-1}\mathbf{g}} \tag{3.5}$$

We note that the inverse is symmetric but not hermitian.

The adiabatic approximation is also very useful during storage, where we are interested in the map from the incoming light to the spin wave. From Eq. (3.1) we see that the equation which relates $\mathcal{E}_{\text{in}}$ and $\mathbf{v}$ in the adiabatic approximation is

$$\dot{\mathbf{s}} = -\mathbf{A}\mathbf{s} - \mathcal{E}_{\text{in}}\mathbf{w} \quad \text{with} \quad \mathbf{w} = i\sqrt{\frac{2}{\kappa}}\mathbf{\Omega}^\dagger\mathbf{\Gamma}^{-1}\mathbf{g}. \tag{3.6}$$

3.1 Time dependence of control beam

The adiabatic approximation in the equations of motions leading to Eq. (3.3) makes it useful to formulate the equations of motions independent of the time-varying amplitude of the control beam $\Omega(t)$. Because all atoms in the cavity are interacting with the same control beam, we can separate the time dependent part from the time independent part in $\mathbf{\Omega}$ such that $\mathbf{\Omega}(t) = \Omega(t)\boldsymbol{\xi}$. Introducing

$$h(t, t') = \int_t^{t'} |\Omega(t'')|^2 dt'' \tag{3.7}$$

together with the rescaled variable $\tilde{\mathcal{E}}_{\text{out}}(h(T_r, t)) = \mathcal{E}_{\text{out}}(t)/\Omega(t)$ allows us to make a change of variables $t \to h(T_r, t)$ in Eq. (3.3) such that

$$\begin{aligned} \tilde{\mathcal{E}}_{\text{out}}\left(h\left(T_r, t\right)\right) =& \mathbf{v}^\dagger \mathbf{s}\left(h\left(T_r, t\right)\right) \\ \frac{d\mathbf{s}\left(h\left(T_r, t\right)\right)}{dh(T_r, t)} =& -\boldsymbol{\xi}^\dagger\mathbf{\Gamma}^{-1}\boldsymbol{\xi}\mathbf{s}\left(h\left(T_r, t\right)\right). \end{aligned} \tag{3.8}$$

The spin wave and the rescaled outgoing field are then the matrix exponentials

$$\mathbf{s}\left(h\left(T_r, t\right)\right) = \exp\left[-\boldsymbol{\xi}^\dagger\mathbf{\Gamma}^{-1}\boldsymbol{\xi}h\left(T_r, t\right)\right]\mathbf{s}\left(h\left(-\infty, T_r\right)\right) \tag{3.9}$$

$$\tilde{\mathcal{E}}_{\text{out}}\left(h\left(T_r, t\right)\right) = -\sqrt{\frac{2}{\kappa}}\mathbf{g}^T\mathbf{\Gamma}^{-1}\boldsymbol{\xi}\exp\left[-\boldsymbol{\xi}^\dagger\mathbf{\Gamma}^{-1}\boldsymbol{\xi}h\left(T_r, t\right)\right]\mathbf{s}\left(h\left(-\infty, T_r\right)\right). \tag{3.10}$$

Consequently the retrieval efficiency η_r can then be written as an integral over the new variable $h(T_r, t)$ such that

$$\begin{aligned}\eta_r =& \int_0^{h(T_r,\infty)} |\tilde{\mathcal{E}}_{\text{out}}\left(h\left(T_r,t\right)\right)|^2 dh(T_r,t) \\ =& \frac{2}{\kappa}\int_0^{h(T_r,\infty)} \left|\mathbf{g}^T\boldsymbol{\Gamma}^{-1}\boldsymbol{\xi}\exp\left[-\boldsymbol{\xi}^\dagger\boldsymbol{\Gamma}^{-1}\boldsymbol{\xi}h\left(T_r,t\right)\right]\mathbf{s}\left(h\left(-\infty,T_r\right)\right)\right|^2 dh(T_r,t) \end{aligned} \quad (3.11)$$

and showing that the retrieval efficiency in the adiabatic approximation is independent of the control beam shape $\Omega(t)$ during retrieval.

During storage we can show that the stored spin wave $\mathbf{s}\left(h\left(-\infty,T_r\right)\right)$ is independent of the time varying control beam amplitude if the ingoing field is rescaled in the same fashion as the outgoing field $\tilde{\mathcal{E}}_{\text{in}}(h(-\infty,t)) = \mathcal{E}_{\text{in}}(t)/\Omega(t)$. Making the change of variables $t \to h(-\infty,t)$ in Eq. (3.6) leads to

$$\frac{d\mathbf{s}\left(h\left(-\infty,t\right)\right)}{dh(-\infty,t)} = \boldsymbol{\xi}^\dagger\boldsymbol{\Gamma}^{-1}\boldsymbol{\xi}\mathbf{s}\left(h\left(-\infty,t\right)\right) + i\sqrt{\frac{2}{\kappa}}\tilde{\mathcal{E}}_{\text{in}}\left(h\left(-\infty,t\right)\right)\boldsymbol{\xi}^\dagger\boldsymbol{\Gamma}^{-1}\mathbf{g}. \quad (3.12)$$

After storage of the quantum field has been completed at time T the spin wave in terms of the rescaled variable $\tilde{\mathcal{E}}_{\text{in}}$ is given by

$$\begin{aligned}\mathbf{s}\left(h\left(-\infty,T\right)\right) =& -\sqrt{\frac{2}{\kappa}}\int_0^{h(-\infty,T)} dh\left(-\infty,t\right) \\ & \times\exp\left[-\boldsymbol{\xi}^\dagger\boldsymbol{\Gamma}^{-1}\boldsymbol{\xi}\left(h\left(-\infty,T\right)-h\left(-\infty,t\right)\right)\right]\boldsymbol{\xi}^\dagger\boldsymbol{\Gamma}^{-1}\mathbf{g}\tilde{\mathcal{E}}_{\text{in}}\left(h\left(-\infty,t\right)\right).\end{aligned} \quad (3.13)$$

These results show that there is a one-to-one correspondence between the rescaled light field and the spin wave, meaning between $\tilde{\mathcal{E}}_{\text{in}}$ and $\mathbf{s}\left(h\left(-\infty,T\right)\right)$ during storage and between $\mathbf{s}\left(h\left(-\infty,T_r\right)\right)$ and $\tilde{\mathcal{E}}_{\text{out}}$ during retrieval, for systems with fixed distributions $\{g^{(i)}\}$, $\{\Omega^{(i)}\}$ and $\{\Delta^{(i)}\}$. We can see that $\tilde{\mathcal{E}}_{\text{in}}$ always is independent of a specific control beam shape $\Omega(t)$. If we for example have found $\tilde{\mathcal{E}}_{\text{in max}}$ from a combination $\Omega(t)_{\text{max}}$, $\mathcal{E}_{\text{in}\max}$ which stores on the spin wave from which we can retrieve with the maximum retrieval efficiency, we can always get the same result for a different $\mathcal{E}'_{\text{in}}$ if a different control beam is used $\Omega'(t) = \Omega_1(t)\mathcal{E}'_{\text{in}}(t)/\mathcal{E}_{\text{in}\max}(t)$. This is very useful in our calculations, because we in Eq. (3.1) just can assume $\boldsymbol{\Omega}$ to be time independent, calculate relevant quantities and subsequently perform a rescaling

$$\mathcal{E}_{\text{in}}(t) \to \frac{\mathcal{E}_{\text{in}}(t)}{\Omega(t)} \quad \text{and} \quad \mathcal{E}_{\text{out}}(t) \to \frac{\mathcal{E}_{\text{out}}(t)}{\Omega(t)} \quad (3.14)$$

to generalize the result for all $\mathcal{E}_{\text{in}}$ and $\mathcal{E}_{\text{out}}$.

3.2 Numerical solution for retrieval

In this section we will show how to numerically calculate the retrieval efficiency when inhomogeneities are included in the model and how to find the maximum retrieval efficiency. This method can be used for any distribution of $\{g^{(i)}\}$, $\{\Omega^{(i)}\}$ and $\{\Delta^{(i)}\}$.

We start with Eq. (3.3), which describes the dynamics of the spin wave. As we have shown in the previous section, we can assume the Rabi oscillations in $\mathbf{\Omega}$ to be time-independent such that the spin wave is the matrix exponential $\mathbf{s} = e^{-\mathbf{A}t}\mathbf{s}(0)$. The outgoing field is then of the simple form $\mathcal{E}_{\text{out}}(t) = \mathbf{v}^\dagger e^{-\mathbf{A}t}\mathbf{s}(0)$ when retrieval starts at $T_r = 0$. Furthermore, we take the absolute square and integrate to find the retrieval efficiency

$$\eta_r = \int_0^\infty dt\, \mathbf{s}^\dagger(0) e^{-\mathbf{A}^\dagger t}\mathbf{v}\mathbf{v}^\dagger e^{-\mathbf{A}t}\mathbf{s}(0). \tag{3.15}$$

The integral is then solved by making the Ansatz

$$\mathbf{M}(t) = \int_0^t dt'\, e^{-\mathbf{A}^\dagger t'}\mathbf{v}\mathbf{v}^\dagger e^{-\mathbf{A}t'} = e^{-\mathbf{A}^\dagger t}\mathbf{C}^\dagger\mathbf{v}\mathbf{v}^\dagger\mathbf{C}e^{-\mathbf{A}t} \tag{3.16}$$

such that we have to determine $\mathbf{C}$ or hermitian $\mathbf{B} = \mathbf{C}^\dagger\mathbf{v}\mathbf{v}^\dagger\mathbf{C}$. Differentiating both the left-hand side and the right-hand side of the previous equation results then in

$$\dot{\mathbf{M}}(t) = e^{-\mathbf{A}^\dagger t}\mathbf{v}\mathbf{v}^\dagger e^{-\mathbf{A}t} = -e^{-\mathbf{A}^\dagger t}\mathbf{A}^\dagger\mathbf{B}e^{-\mathbf{A}t} - e^{-\mathbf{A}^\dagger t}\mathbf{B}\mathbf{A}e^{-\mathbf{A}t}. \tag{3.17}$$

When we exclude the exponential functions, we see that the problem is reduced to solving the so-called Sylvester equation

$$-\mathbf{A}^\dagger\mathbf{B} - \mathbf{B}\mathbf{A} = \mathbf{v}\mathbf{v}^\dagger \tag{3.18}$$

for $\mathbf{B}$, because both $\mathbf{A}$ and $\mathbf{v}$ are specified by the parameters of the quantum memory. There exist numerous numeric algorithms to solve the Sylvester equation. Not surprisingly, numerical solutions become increasingly difficult for increasing N. When we have found $\mathbf{B}$, we can find the retrieval efficiency through

$$\eta_r = \mathbf{s}^\dagger(0)[\mathbf{M}(t)]_0^\infty\mathbf{s}(0) = \mathbf{s}^\dagger(0)\,(-\mathbf{B})\,\mathbf{s}(0). \tag{3.19}$$

We note that the maximum eigenvalue of $-\mathbf{B}$ corresponds to the maximum retrieval efficiency. This can be shown by using the variational principle. The hermitian matrix $-\mathbf{B}$ has the decomposition

$$-\mathbf{B} = \sum_i \lambda_i \mathbf{u}_i\mathbf{u}_i^\dagger \tag{3.20}$$

with eigenvalues λ_i and orthonormal eigenvectors $\mathbf{u}_k$. For a spin wave expanded as $\mathbf{s}(0) = \sum_i \alpha_i\mathbf{u}_i$ the retrieval efficiency has the upper bound

$$\eta_r = \sum_i \lambda_i|\alpha_i|^2 \leq \lambda_{\max}\sum_i |\alpha_i|^2 = \lambda_{\max} \tag{3.21}$$

because we assume that $\mathbf{s}(0)^\dagger\mathbf{s}(0) = \sum_i |\alpha_i|^2 = 1$ when calculating the retrieval efficiency. Furthermore we know that the maximum retrieval efficiency is attained for the spin wave $\mathbf{s} = \mathbf{u}_{\max}$ where $\mathbf{u}_{\max}$ is the eigenvector with the corresponding eigenvalue $\lambda_{\max}$.

In Figure 3.1 we have calculated the maximum retrieval efficiency for three different continuous distribution, a Gaussian, a Lorentzian and a Uniform distribution with

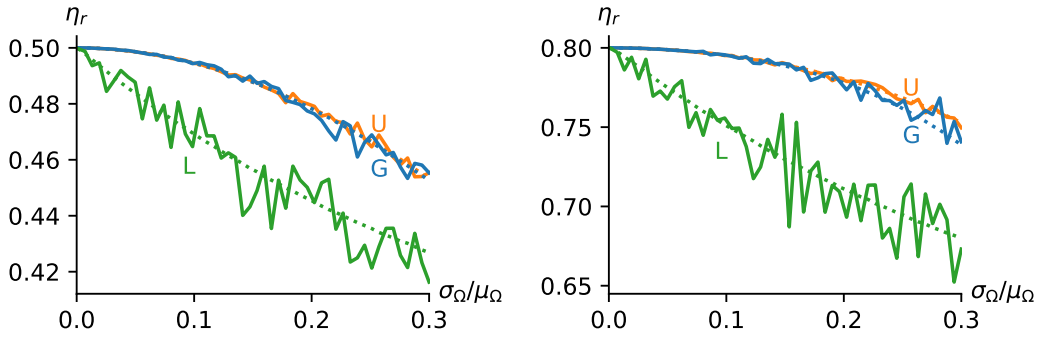

Figure 3.1: Maximum retrieval efficiency as a function of the scale divided by mean value of (G) Gaussian, (L) Lorentzian and (U) uniform distributions for $\{\Omega^{(i)}\}$. For the Gaussian profile the standard deviation σ_Ω and for the Lorentzian profile the half width at half maximum y is used as scale. The scale of the uniform profile is $w/3.5 \approx \sigma_\Omega$. In (a) we retrieve from a system with $C = 1$ and in (b) from a system with $C = 4$.

the following probability density functions:

$$f_G(\Omega) = \frac{1}{2\pi\sigma_\Omega} \exp\left(-\frac{(\Omega - \mu_\Omega)^2}{2\sigma_\Omega^2}\right) \tag{3.22}$$

$$f_L(\Omega) = \frac{1}{\pi} \frac{y}{(\Omega - \mu_\Omega)^2 + y^2} \tag{3.23}$$

$$f_U(\Omega) = \begin{cases} \frac{1}{w} & \text{for } \mu_\Omega - \frac{w}{2} \leq \Omega \leq \mu_\Omega + \frac{w}{2} \\ 0 & \text{otherwise} \end{cases} \tag{3.24}$$

We draw the random samples $\{\Omega^{(i)}\}$ from these continuous distributions, while keeping $\{g^{(i)}\}$ and $\{\Delta^{(i)}\}$ homogeneous. The size of the atomic ensemble has been set to $N = 200$ in the calculations. The solid lines represent the retrieval efficiency for a random sample. Because the size of the atomic ensemble $N = 200$ is relatively small in these calculations, there are variations in the retrieval efficiency for different random samples drawn from the same distribution. When the retrieval efficiency is calculated for a different scale factor of the distribution, a new random sample has to be drawn, which leads to fluctuations. This is a result of the quenched disorder of the system, which a system exhibits when some defining parameters are random variables and they do not change with time. The system does therefore not evolve toward some kind of expected state during retrieval for different random samples drawn from the same distribution, making it more difficult to analyze its behavior. In order to calculate a non-fluctuating average of the retrieval efficiency, the average has to be taken with respect to a very large number of calculations. However, this can already be very time consuming for small samples with $N = 200$. Instead of calculating averages, we therefore have included the retrieval efficiency for an "ideal" sample (dotted line). The maximum value of this sample is set equal to the average maximum value of a random sample, the second-highest value of this sample is set

equal to the average second highest value of a random sample and so on. It does then have many of the same properties as the continuous distribution.

The results in Figure 3.1 show that the retrieval efficiency decreases when the distributions broaden. When comparing the results in (a) and (b) we see that the retrieval efficiency decreases more rapidly in (b), where the system has the higher maximum retrieval efficiency. Moreover, we see that the retrieval efficiency has very similar dependence on the standard deviation for the Gaussian and the Uniform distributions in both (a) and (b). The scale of the uniform distribution is varied as $w/3.5 \approx \sigma_\Omega$, which approximately is equal to the standard deviation of the uniform distribution. However, it is not possible to adjust the scale of the Lorentzian profile such that the curve fits the other distributions. While the maximal retrieval efficiency for small broadening seems to have a second order dependence for the Gaussian and Uniform distributions, it seems to have a first order dependence for the Lorentzian distribution. We do therefore conclude that systems with Lorentzian inhomogeneity profiles have a qualitative different behavior with regard to the maximal retrieval efficiency than systems with Gaussian and uniform inhomogeneity profiles. In the next chapter we are going to focus on distributions with well-defined moments, such as Gaussian and uniform distributions, when trying to find a symbolic expression for the retrieval efficiency.

Chapter 4

Optimization of retrieval

In order to obtain general results of the conditions in which efficient retrieval with the quantum memory is possible, it is desirable to find an symbolic expression of the retrieval efficiency. Generally it is very difficult to diagonalize the matrix $\mathbf{A}$ in Eq. (3.3) which gives the outgoing field $\mathcal{E}_{\text{out}}(t) = \mathbf{v}^\dagger e^{-\mathbf{A}t}\mathbf{s}(0)$ and we therefore have to rely on approximate techniques. In this chapter, we present a method which allows us to write the retrieval efficiency as a series expansion, where the terms depend on the moments of the different distributions. For this method to be suitable, it is therefore a requirement that all moments are well defined. After having introduced the method, we look specifically at the retrieval efficiency for Gaussian distributions of $\{g^{(i)}\}$, $\{\Omega^{(i)}\}$ and $\{\Delta^{(i)}\}$, where we can expand $\mathcal{E}_{\text{out}}(t)$ as a series with respect to the standard deviation of the different distributions. In order to simplify the calculations we will look separately at inhomogeneities with $\{g^{(i)}\}$ and $\{\Omega^{(i)}\}$ and inhomogeneous broadening. Furthermore we characterize the spin wave which allows for maximum retrieval, because this allows us to draw conclusions about how the conditions for optimal retrieval also are valid for optimizing the whole process of both storage and retrieval.

4.1 Model

4.1.1 Krylov subspace and Arnoldi iteration

The matrix exponential function $\mathbf{v}^\dagger e^{-\mathbf{A}t}$ can be expanded as power series, generating terms with $\mathbf{v}^\dagger, \mathbf{v}^\dagger\mathbf{A}, \mathbf{v}^\dagger\mathbf{A}^2$ and so on. All these terms are linearly independent when inhomogeneities in $\{\Omega^{(i)}\}$ or $\{\Delta^{(i)}\}$ are included in the model and we can therefore create the so-called n'th order Krylov subspace [36, 37]

$$\mathcal{K}_n = \text{span}\left\{\mathbf{v}, \mathbf{A}\mathbf{v}, \mathbf{A}^2\mathbf{v}, \ldots, \mathbf{A}^{n-1}\mathbf{v}\right\}. \tag{4.1}$$

Our aim is now to build an orthonormal basis with n vectors $\{\mathbf{e}_0, \mathbf{e}_1, \ldots, \mathbf{e}_{n-1}\}$ from this subspace such that we can approximate the matrix exponential $\mathcal{E}_{\text{out}}(t)$ up to terms which depend on $\mathbf{v}^\dagger\mathbf{A}^{n-1}$. We can find the orthonormal basis with the help of an so-called Arnoldi iteration, which basically amounts to applying the Gram-Schmidt orthogonalization to the Krylov subspace. According to the iteration, the

first normalized basis vector is simply

$$\mathbf{e}_0^\dagger = \mathbf{v}^\dagger / \sqrt{\mathbf{v}^\dagger \mathbf{v}} \tag{4.2}$$

Afterwards we orthogonalize $\mathbf{A}\mathbf{e}_0$ against $\mathbf{e}_0$ in order to find the next basis vector.

$$\mathbf{u}_1^\dagger = \mathbf{e}_0^\dagger \mathbf{A} - \mathbf{e}_0^\dagger \mathbf{A} \mathbf{e}_0 \mathbf{e}_0^\dagger \tag{4.3}$$

$$\mathbf{e}_1^\dagger = \frac{\mathbf{u}_1^\dagger}{\sqrt{\mathbf{u}_1^\dagger \mathbf{u}_1}} = \frac{\mathbf{e}_0^\dagger \mathbf{A} \left(1 - \mathbf{e}_0 \mathbf{e}_0^\dagger\right)}{\left[\mathbf{e}_0^\dagger \mathbf{A} \left(1 - \mathbf{e}_0 \mathbf{e}_0^\dagger\right) \left(1 - \mathbf{e}_0 \mathbf{e}_0^\dagger\right) \mathbf{A}^\dagger \mathbf{e}_0\right]^{1/2}} \tag{4.4}$$

This iteration is continued in the same manner until the n'th normalized basis vector is found.

$$\mathbf{u}_{n-1}^\dagger = \mathbf{e}_{n-2}^\dagger \mathbf{A} - \sum_{i=0}^{n-2} \mathbf{e}_{n-2}^\dagger \mathbf{A} \mathbf{e}_i \mathbf{e}_i^\dagger \qquad \mathbf{e}_{n-1}^\dagger = \frac{\mathbf{u}_{n-1}^\dagger}{\sqrt{\mathbf{u}_{n-1}^\dagger \mathbf{u}_{n-1}}} \tag{4.5}$$

Having created an orthonormal basis, we see that the outgoing field can be written in terms of the spin-wave mode $s_0(t) = \mathbf{e}_0^\dagger \mathbf{s}(t)$ such that

$$\mathcal{E}_{\text{out}}(t) = \sqrt{\mathbf{v}^\dagger \mathbf{v}} s_0(t) \quad \text{and} \quad \eta_r = \mathbf{v}^\dagger \mathbf{v} \int_{T_r}^{\infty} |s_0(t)|^2 dt. \tag{4.6}$$

Without inhomogeneities in $\{\Omega^{(i)}\}$ or $\{\Delta^{(i)}\}$ the spin-wave can be described by one collective mode $s_0(t)$ leading to an retrieval efficiency of $\eta_r = C/(1+C)$ as described previously. However, with small inhomogeneities included in the system other modes couple to this mode, leading to a variation in the result.

Now the task is to find a solution to $s_0(t)$ by transforming the differential equation $\dot{\mathbf{s}} = -\mathbf{A}\mathbf{s}$ from Eq. (3.3) with the orthonormal basis. Multiplying with $\mathbf{e}_0^\dagger$ on both sides of the differential equation results in the derivative $\dot{s}_0 = -\mathbf{e}_0^\dagger \mathbf{A} \mathbf{s}$ such that when inserting $1 - \mathbf{e}_0 \mathbf{e}_0^\dagger + \mathbf{e}_0 \mathbf{e}_0^\dagger$ we have

$$\dot{s}_0 = -\mathbf{e}_0^\dagger \mathbf{A} \left(1 - \mathbf{e}_0 \mathbf{e}_0^\dagger\right) \mathbf{s} - \mathbf{e}_0^\dagger \mathbf{A} \mathbf{e}_0 \mathbf{e}_0^\dagger \mathbf{s}. \tag{4.7}$$

The first term is only nonzero when inhomogeneities in $\left\{\Omega^{(i)}\right\}$ or $\left\{\Delta^{(i)}\right\}$ are included in the model (where $\mathbf{e}_0 \propto \mathbf{g}$ and $\mathbf{A} \propto a\mathbf{I} - \mathbf{g}\mathbf{g}^\dagger$ with a being a constant) and it depends on the coupling of the symmetric mode to a second mode, while the second term gives the zeroth order contribution to the retrieval efficiency we determined previously. Defining the second mode as $s_1(t) = \mathbf{e}_1^\dagger \mathbf{s}(t)$ allows us to redefine Eq. (4.7) in terms of the two modes and their coupling.

$$\dot{s}_0 = -k_{01} s_1 - k_{00} s_0 \tag{4.8}$$

Here, the constants are simply $k_{00} = \mathbf{e}_0^\dagger \mathbf{A} \mathbf{e}_0$ and $k_{01} = \mathbf{e}_0^\dagger \mathbf{A} \mathbf{e}_1$. We note that the coefficient k_{01} corresponds to the denominator in Eq. (4.4) and therefore always is real. This method can now in principle be continued endlessly, because there exist an infinite number of spin-wave modes. The derivative of the next mode is found to be

$$\begin{aligned} \dot{s}_1 &= -\mathbf{e}_1^\dagger \mathbf{A} \left(1 - \mathbf{e}_0 \mathbf{e}_0^\dagger - \mathbf{e}_1 \mathbf{e}_1^\dagger\right) \mathbf{s} - \mathbf{e}_1^\dagger \mathbf{A} \mathbf{e}_0 \mathbf{e}_0^\dagger \mathbf{s} - \mathbf{e}_1^\dagger \mathbf{A} \mathbf{e}_1 \mathbf{e}_1^\dagger \mathbf{s} \\ &= -k_{12} s_2 - k_{10} s_0 - k_{11} s_1. \end{aligned} \tag{4.9}$$

Again the first term couples to a higher order spin wave mode. The constants are given by $k_{12} = \mathbf{e}_1^\dagger \mathbf{A} \mathbf{e}_2$ and $k_{11} = \mathbf{e}_1^\dagger \mathbf{A} \mathbf{e}_1$. The derivative of the n'th mode is then accordingly

$$\begin{aligned} \dot{s}_n &= -\mathbf{e}_n^\dagger \mathbf{A} \left(1 - \sum_{i=0}^{n} \mathbf{e}_n \mathbf{e}_n^\dagger \right) \mathbf{s} - \sum_{i=0}^{n} \mathbf{e}_n^\dagger \mathbf{A} \mathbf{e}_i \mathbf{e}_i^\dagger \\ &= -\mathbf{e}_{n+1}^\dagger \mathbf{A} \mathbf{e}_i \mathbf{s} - \sum_{i=0}^{n} k_{ni} s_i \end{aligned} \tag{4.10}$$

where $k_{ni} = \mathbf{e}_n^\dagger \mathbf{A} \mathbf{e}_i$. Because $\sum_{i=0}^{n} \mathbf{e}_n \mathbf{e}_n^\dagger \to \mathbf{I}$ for $n \to \infty$, we expect the firts term $k_{n,n+1} s_{n+1}$ to become smaller with increasing n. If $\mathcal{K}_m$ is the Krylov subspace which spans a large part of the entire space and $\mathcal{K}_n$ is a Krylov subspace which spans a smaller part of the entire space, we have now transformed the differential equation $\dot{\mathbf{s}} = -\mathbf{A}\mathbf{s}$ into a system with a lower Hessenberg matrix.

$$\begin{pmatrix} \dot{s}_0 \\ \dot{s}_1 \\ \\ \vdots \\ \\ \\ \dot{s}_n \\ \vdots \\ \dot{s}_m \end{pmatrix} = - \begin{pmatrix} k_{00} & k_{01} & 0 & & \dots & & & 0 \\ k_{10} & k_{11} & k_{12} & 0 & \dots & & & \\ & & k_{22} & k_{23} & \ddots & & & \\ \vdots & \vdots & \vdots & & \ddots & 0 & & \vdots \\ & & & & & k_{n-1,n} & \ddots & \\ k_{n0} & k_{n1} & k_{n2} & & \dots & k_{n,n} & \ddots & 0 \\ \vdots & \vdots & \vdots & & & & \ddots & k_{m-1,m} \\ k_{m0} & k_{m1} & k_{m2} & & \dots & & & k_{mm} \end{pmatrix} \begin{pmatrix} s_0 \\ s_1 \\ \\ \vdots \\ \\ \\ s_n \\ \vdots \\ s_m \end{pmatrix} \tag{4.11}$$

When the term $k_{n,n+1} s_{n+1}$ is sufficiently small, it is no longer necessary to work in a basis which includes m basis vectors and we can reduce the system to the subspace $\mathcal{K}_n$.

$$\begin{pmatrix} \dot{s}_0 \\ \dot{s}_1 \\ \\ \vdots \\ \\ \dot{s}_n \end{pmatrix} = - \begin{pmatrix} k_{00} & k_{01} & 0 & & \dots & 0 \\ k_{10} & k_{11} & k_{12} & 0 & \dots & \\ & & k_{22} & k_{23} & \ddots & \\ \vdots & \vdots & \vdots & & \ddots & 0 \\ & & & & & k_{n-1,n} \\ k_{n0} & k_{n1} & k_{n2} & & \dots & k_{n,n} \end{pmatrix} \begin{pmatrix} s_0 \\ s_1 \\ \\ \vdots \\ \\ s_n \end{pmatrix} \tag{4.12}$$

This is equal to $\mathbf{Q}_n \dot{\mathbf{s}} = \mathbf{Q}_n \mathbf{A} \mathbf{Q}_n^\dagger \mathbf{Q}_n \mathbf{s}$ with $\mathbf{Q}_n = (\mathbf{e}_0\, \mathbf{e}_1\, \dots\, \mathbf{e}_n)$, where the system is projected orthogonally onto the subspace $\mathcal{K}_n$. We can now find $s_0(t)$ in the reduced subspace $\mathcal{K}_n$ and use Eq. (4.6) to calculate the retrieval efficiency.

4.1.2 Retrieval efficiency for $\mathcal{K}_2$ subspace

We will now try to derive the retrieval efficiency for the most simple subspace which includes contributions of the inhomogeneities in $\{\Omega^{(i)}\}$ and $\{\Delta^{(i)}\}$. The differential equation is in this case reduced to

$$\begin{pmatrix} \dot{s}_0 \\ \dot{s}_1 \end{pmatrix} = - \begin{pmatrix} k_{00} & k_{01} \\ k_{10} & k_{11} \end{pmatrix} \begin{pmatrix} s_0 \\ s_1 \end{pmatrix}. \tag{4.13}$$

If the inhomogeneities are denotes as deviations from the mean value such that $\Omega^{(i)} = \langle\Omega\rangle + \delta\Omega^{(i)}$ and $\Delta^{(i)} = \langle\Delta\rangle + \delta\Delta(i)$, the subspace $\mathcal{K}_2$ includes all second-order contributions of the inhomogeneities, $\sum_i {\delta\Omega^{(i)}}^2$, $\sum_i {\delta\Delta^{(i)}}^2$ and so on. For small inhomogeneities it is often sufficient to only include these lowest order contributions to the retrieval efficiency and therefore sufficient to project the system onto $\mathcal{K}_2$. In order to find the lowest order contribution of the inhomogeneities to the retrieval efficiency, we have to find out how the coefficient matrix is related to the different distributions. This relation is determined by the moments of the different distributions with known $\mathbf{g}$, $\mathbf{\Omega}$ and $\mathbf{\Delta}$. Assuming $\mathbf{g}$ and $\mathbf{\Omega}$ to be real for simplicity, we will use the following notation for the sum

$$\left\langle g^k \Omega^l |\tilde{\Delta}|^{-m} \tilde{\Delta}^{-n} \right\rangle = \frac{1}{N} \sum_{i=1}^{N} \sum_{j=e_1 \ldots e_N} \frac{{g_j^{(i)}}^k {\Omega_j^{(i)}}^l}{\left|\gamma + i\Delta_j^{(i)}\right|^m \left(\gamma + i\Delta_j^{(i)}\right)^n} \tag{4.14}$$

which depends on the moments of the different samples. Already previously in Eq. (3.4), we have found $\mathbf{v}$ and $\mathbf{A}$ in terms of the elements of the different distributions.

$$\mathbf{v}^\dagger = -a\sqrt{\frac{2}{\kappa}} \mathbf{g}^T \tilde{\mathbf{\Delta}}^{-1} \mathbf{\Omega} \qquad \mathbf{A} = \mathbf{\Omega}\tilde{\mathbf{\Delta}}^{-1}\mathbf{\Omega} - \frac{\mathbf{\Omega}\tilde{\mathbf{\Delta}}^{-1}\mathbf{g}\mathbf{g}^T\tilde{\mathbf{\Delta}}^{-1}\mathbf{\Omega}}{\kappa + N\left\langle g^2 \tilde{\Delta}^{-1} \right\rangle} \tag{4.15}$$

Here we have defined the prefactor

$$a = \frac{\kappa}{\kappa + N\left\langle g^2 \tilde{\Delta}^{-1} \right\rangle}. \tag{4.16}$$

This allows us then to find the first two basis vectors from the Arnoldi iteration in terms of the elements of the distributions using Eq. (4.2) and (4.4).

$$\mathbf{e}_0^\dagger = \frac{a}{|a|} \frac{\mathbf{g}^T \tilde{\mathbf{\Delta}}^{-1} \mathbf{\Omega}}{\sqrt{N\left\langle g^2 \Omega^2 |\tilde{\Delta}|^{-2} \right\rangle}} \tag{4.17}$$

$$\mathbf{e}_1^\dagger = \frac{a}{|a|} \frac{\left\langle g^2\Omega^2|\tilde{\Delta}|^{-2}\right\rangle \mathbf{g}^T \left(\tilde{\mathbf{\Delta}}^{-1}\right)^2 \mathbf{\Omega}^3 - \left\langle g^2\Omega^4|\tilde{\Delta}|^{-2}\tilde{\Delta}^{-1}\right\rangle \mathbf{g}^T\tilde{\mathbf{\Delta}}^{-1}\mathbf{\Omega}}{\sqrt{N}\left(\left\langle g^2\Omega^2|\tilde{\Delta}|^{-2}\right\rangle^2 \left\langle g^2\Omega^6|\tilde{\Delta}|^{-4}\right\rangle - \left\langle g^2\Omega^2|\tilde{\Delta}|^{-2}\right\rangle \left|\left\langle g^2\Omega^4|\tilde{\Delta}|^{-2}\tilde{\Delta}^{-1}\right\rangle\right|^2\right)^{1/2}} \tag{4.18}$$

It is a little bit more convenient to have a definition of the basis vectors which does not include the prefactor $a/|a|$. We therefore absorb the prefactor into the definition of $\mathcal{E}_{\text{out}}(t)$, which forces us to redefine in Eq. (4.6) how the outgoing field is related to the mode $s_0(t) = \mathbf{e}_0^\dagger \mathbf{s}(t)$ such that

$$\mathcal{E}_{\text{out}}(t) = \frac{a}{|a|}\sqrt{\mathbf{v}^\dagger\mathbf{v}}\, s_0(t). \tag{4.19}$$

The first two orthonormal basis vectors in the Arnoldi iteration are then

$$\mathbf{e}_0^\dagger = \frac{\mathbf{g}^T \tilde{\mathbf{\Delta}}^{-1} \mathbf{\Omega}}{\sqrt{N \left\langle g^2 \Omega^2 |\tilde{\Delta}|^{-2} \right\rangle}} \tag{4.20}$$

$$\mathbf{e}_1^\dagger = \frac{\left\langle g^2\Omega^2|\tilde{\Delta}|^{-2}\right\rangle \mathbf{g}^T \left(\tilde{\mathbf{\Delta}}^{-1}\right)^2 \mathbf{\Omega}^3 - \left\langle g^2\Omega^4|\tilde{\Delta}|^{-2}\tilde{\Delta}^{-1}\right\rangle \mathbf{g}^T \tilde{\mathbf{\Delta}}^{-1}\mathbf{\Omega}}{\sqrt{N}\left(\left\langle g^2\Omega^2|\tilde{\Delta}|^{-2}\right\rangle^2 \left\langle g^2\Omega^6|\tilde{\Delta}|^{-4}\right\rangle - \left\langle g^2\Omega^2|\tilde{\Delta}|^{-2}\right\rangle \left|\left\langle g^2\Omega^4|\tilde{\Delta}|^{-2}\tilde{\Delta}^{-1}\right\rangle\right|^2\right)^{1/2}}. \tag{4.21}$$

For the purpose of calculating retrieval efficiencies this definition does not change anything. Because we integrate over the absolute square of the outgoing field when finding the retrieval efficiency, the prefactor disappears $\eta_r = \int_{T_r}^{\infty} |\mathcal{E}_{\text{out}}(t)|^2 dt = \mathbf{v}^\dagger\mathbf{v} \int_{T_r}^{\infty} |s_0(t)|^2 dt$.

Having defined the first two basis vectors allows us now to find the first four coefficients in terms of the moments through $k_{ij} = \mathbf{e}_i^\dagger \mathbf{A} \mathbf{e}_j$.

$$k_{00} = \frac{\left\langle g^2\Omega^4|\tilde{\Delta}|^{-2}\tilde{\Delta}^{-1}\right\rangle}{\left\langle g^2\Omega^2|\tilde{\Delta}|^{-2}\right\rangle} - \frac{N\left\langle g^2\Omega^2\tilde{\Delta}^{-2}\right\rangle}{\kappa + N\left\langle g^2\tilde{\Delta}^{-1}\right\rangle}$$

$$k_{01} = \left(\frac{\left\langle g^2\Omega^6|\tilde{\Delta}|^{-4}\right\rangle}{\left\langle g^2\Omega^2|\tilde{\Delta}|^{-2}\right\rangle} - \frac{\left|\left\langle g^2\Omega^4|\tilde{\Delta}|^{-2}\tilde{\Delta}^{-1}\right\rangle\right|^2}{\left\langle g^2\Omega^2|\tilde{\Delta}|^{-2}\right\rangle^2}\right)^{1/2} \tag{4.22}$$

$$\begin{aligned} k_{10} = &\left(\left\langle g^2\Omega^2|\tilde{\Delta}|^{-2}\right\rangle^3 \left\langle g^2\Omega^6|\tilde{\Delta}|^{-4}\right\rangle - \left\langle g^2\Omega^2|\tilde{\Delta}|^{-2}\right\rangle^2 \left|\left\langle g^2\Omega^4|\tilde{\Delta}|^{-2}\tilde{\Delta}^{-1}\right\rangle\right|^2\right)^{-1/2} \\ &\times \left[\left\langle g^2\Omega^2|\tilde{\Delta}|^{-2}\right\rangle \left\langle g^2\Omega^6|\tilde{\Delta}|^{-2}\tilde{\Delta}^{-2}\right\rangle - \left\langle g^2\Omega^4|\tilde{\Delta}|^{-2}\tilde{\Delta}^{-1}\right\rangle^2 \right. \\ &\left. + N\frac{\left\langle g^2\Omega^4|\tilde{\Delta}|^{-2}\tilde{\Delta}^{-1}\right\rangle \left\langle g^2\Omega^2|\tilde{\Delta}|^{-2}\right\rangle \left\langle g^2\Omega^2\tilde{\Delta}^{-2}\right\rangle - \left\langle g^2\Omega^2|\tilde{\Delta}|^{-2}\right\rangle^2 \left\langle g^2\Omega^4\tilde{\Delta}^{-3}\right\rangle}{\kappa + N\left\langle g^2\tilde{\Delta}^{-1}\right\rangle}\right] \end{aligned} \tag{4.23}$$

$$\begin{aligned} k_{11} = &\left(\left\langle g^2\Omega^2|\tilde{\Delta}|^{-2}\right\rangle^2 \left\langle g^2\Omega^6|\tilde{\Delta}|^{-4}\right\rangle - \left\langle g^2\Omega^2|\tilde{\Delta}|^{-2}\right\rangle \left|\left\langle g^2\Omega^4|\tilde{\Delta}|^{-2}\tilde{\Delta}^{-1}\right\rangle\right|^2\right)^{-1} \\ &\times \left[\left\langle g^2\Omega^2|\tilde{\Delta}|^{-2}\right\rangle^2 \left\langle g^2\Omega^8|\tilde{\Delta}|^{-4}\tilde{\Delta}^{-1}\right\rangle - \left\langle g^2\Omega^2|\tilde{\Delta}|^{-2}\right\rangle \left\langle g^2\Omega^4|\tilde{\Delta}|^{-2}\tilde{\Delta}^{*-1}\right\rangle \left\langle g^2\Omega^6|\tilde{\Delta}|^{-2}\tilde{\Delta}^{-2}\right\rangle \right. \\ &\left. - \left\langle g^2\Omega^2|\tilde{\Delta}|^{-2}\right\rangle \left\langle g^2\Omega^4|\tilde{\Delta}|^{-2}\tilde{\Delta}^{-1}\right\rangle \left\langle g^2\Omega^6|\tilde{\Delta}|^{-4}\right\rangle + \left|\left\langle g^2\Omega^4|\tilde{\Delta}|^{-2}\tilde{\Delta}^{-1}\right\rangle\right|^2 \left\langle g^2\Omega^4|\tilde{\Delta}|^{-2}\tilde{\Delta}^{-1}\right\rangle\right] \end{aligned} \tag{4.24}$$

As mentioned before, this approach only works if the moments are well-defined, which for example is not the case for Lorentzian distributions. Furthermore, the inner product $\mathbf{v}^\dagger\mathbf{v}$ includes second-order inhomogeneities, which affect the retrieval

efficiency.

$$\mathbf{v}^\dagger\mathbf{v} = \frac{2N\kappa\left\langle g^2\Omega^2|\tilde{\Delta}|^{-2}\right\rangle}{\left(\kappa + N\left\langle g^2|\tilde{\Delta}|^{-1}\right\rangle\right)^2} \tag{4.25}$$

It is now possible to find a general solution of the retrieval efficiency η_r in $\mathcal{K}_2$, depending on the different moments and the initial spin wave modes $s_1(0)$ and $s_2(0)$.

The time dependence of the spin-wave modes can be found by integrating the differential equations in Eq. (4.13).

$$\begin{aligned} s_0(t) &= e^{-k_{00}t}s_0(0) - k_{01}\int_0^t e^{-k_{00}(t-t')}s_1(t')dt' \\ s_1(t) &= e^{-k_{11}t}s_1(0) - k_{01}\int_0^t e^{-k_{11}(t-t')}s_0(t')dt' \end{aligned} \tag{4.26}$$

Because we expect the contribution from $s_1(t)$ to be lower order compared to the first term in $s_0(t)$, which gives the zeroth order contribution, the differential equation can be solved iteratively:

$$\begin{aligned} s_0(t) =& e^{-k_{00}t}s_0(0) - k_{01}s_1(0)\int_0^t dt' e^{-k_{00}(t-t')}e^{-k_{11}t'} \\ &+ k_{01}k_{10}s_0(0)\int_0^t\int_0^{t'} dt'dt'' e^{-k_{00}(t-t')}e^{-k_{11}(t'-t'')}e^{-k_{00}t''} + \dots \end{aligned} \tag{4.27}$$

Plugging this equation into $\eta_r = \mathbf{v}^\dagger\mathbf{v}\int_{T_r}^\infty |s_0(t)|^2dt$ and calculating the integrals does then give the retrieval efficiency

$$\begin{aligned} \eta_r =& \mathbf{v}^\dagger\mathbf{v}\left\{\frac{|s_0(0)|^2}{2\mathrm{Re}k_{00}} - 2\mathrm{Re}\left[\frac{k_{01}}{k_{11}-k_{00}}s_1(0)s_0^*(0)\left(\frac{1}{2\mathrm{Re}k_{00}} - \frac{1}{k_{11}+k_{00}^*}\right)\right]\right. \\ &\left. +2\mathrm{Re}\left[\frac{k_{01}k_{10}|s_0(0)|^2}{(k_{00}-k_{11})^2}\left(\frac{k_{11}-k_{00}}{4\left(\mathrm{Re}k_{00}\right)^2} - \frac{1}{2\mathrm{Re}k_{00}} + \frac{1}{k_{11}+k_{00}^*}\right)\right]\right\} + \dots \end{aligned} \tag{4.28}$$

where we only have included the dominant term. Let us now denote the order of the inhomogeneities by λ, meaning that $\Omega^{(i)} = \langle\Omega\rangle + \delta\Omega^{(i)}\lambda$, $\Delta^{(i)} = \langle\Delta\rangle + \delta\Delta(i)\lambda$ and $g^{(i)} = \langle g\rangle + \delta g^{(i)}\lambda$. We assume now that $\sum_i \delta\Omega^{(i)} = 0$, $\sum_i \delta\Delta^{(i)} = 0$ and $\sum_i \delta g^{(i)} = 0$, which is true when $\langle\Omega\rangle$, $\langle\Delta\rangle$ and $\langle g\rangle$ denote the sample average values. The elements of the coefficient matrix and $\mathbf{v}^\dagger\mathbf{v}$ can then be expanded as series in terms of λ such that

$$k_{00} = k_{00}^{(0)} + k_{00}^{(2)}\lambda^2 + \mathcal{O}(\lambda^3) \tag{4.29}$$

$$k_{01} = k_{01}^{(1)}\lambda + \mathcal{O}(\lambda^2) \tag{4.30}$$

$$k_{10} = k_{10}^{(1)}\lambda + \mathcal{O}(\lambda^2) \tag{4.31}$$

$$k_{11} = k_{11}^{(0)} + \mathcal{O}(\lambda) \tag{4.32}$$

$$\mathbf{v}^\dagger\mathbf{v} = a^{(0)} + a^{(2)}\lambda^2 + \mathcal{O}(\lambda^3) \tag{4.33}$$

where $k_{00}^{(1)} = k_{01}^{(0)} = k_{10}^{(0)} = a^{(1)} = 0$ because of this assumption. Note that k_{01} and k_{10} includes a first order contribution, which is a sample standard deviation (for

example $\sqrt{\sum_i \delta\Omega^{(i)^2}}$). If we furthermore assume that the spin wave modes at the time $T_r = 0$ of initial retrieval have the following series expansions

$$s_0(0) = s_0^{(0)} + s_0^{(2)}\lambda^2 + \mathcal{O}(\lambda^3) \tag{4.34}$$

$$s_1(0) = s_1^{(1)}\lambda + \mathcal{O}(\lambda^2) \tag{4.35}$$

which are valid because $s_1(0)$ only can couple to $s_0(0)$ to first order, we can find an expression for the retrieval efficiency, that is accurate up to second order in λ. For this we expand Eq. (4.28) by inserting the series expansions such that we find

$$\begin{aligned}\eta_r =& \frac{a^{(0)}|s_0^{(0)}|^2}{2\mathrm{Re}k_{00}^{(0)}} + \frac{a^{(2)}|s_0^{(0)}|^2 - a^{(0)}|s_1^{(1)}|^2}{2\mathrm{Re}k_{00}^{(0)}}\lambda^2 - \frac{a^{(0)}|s_0^{(0)}|^2\mathrm{Re}k_{00}^{(2)}}{2\left(\mathrm{Re}k_{00}^{(0)}\right)^2}\lambda^2 \\ &- \frac{a^{(0)}}{\mathrm{Re}k_{00}^{(0)}}\mathrm{Re}\left[s_0^{(0)^*}s_1^{(1)}\frac{k_{01}^{(1)}\left(k_{00}^{(0)^*} + k_{11}^{(0)} - 2\mathrm{Re}k_{00}^{(0)}\right)}{\left(k_{00}^{(0)^*} + k_{11}^{(0)}\right)\left(k_{11}^{(0)} - k_{00}^{(0)}\right)}\right]\lambda^2 \\ &+ 2a^{(0)}\left|s_0^{(0)}\right|^2\mathrm{Re}\left[\frac{k_{01}^{(1)}k_{10}^{(1)}}{\left(k_{11}^{(0)} - k_{00}^{(0)}\right)^2}\left(\frac{1}{k_{00}^{(0)^*} + k_{11}^{(0)}} + \frac{k_{11}^{(0)} - k_{00}^{(0)}}{4\left(\mathrm{Re}k_{00}^{(0)}\right)^2} - \frac{1}{2\mathrm{Re}k_{00}^{(0)}}\right)\right]\lambda^2 \\ &+ \mathcal{O}\left(\lambda^3\right).\end{aligned} \tag{4.36}$$

Here, the first term is the zeroth order contribution, which we already previously have determined to be equal to $C/(1+C)$.

4.1.3 Optimal retrieval for $\mathcal{K}_2$ subspace

For a given system, the retrieval efficiency can be maximized by retrieving from the right spin wave. We can obtain the optimal retrieval efficiency by maximizing Eq. (4.36) with respect to the initial spin wave modes. Because the number of stored excitations has been set equal to unity $\mathbf{s}^\dagger(0)\mathbf{s}(0) = 1$, the initial spin wave modes are subject to the condition

$$\sum_i |s_i(0)|^2 = |s_0^{(0)}|^2 + 2\mathrm{Re}\left[s_0^{(0)}s_0^{(2)}\right]\lambda^2 + |s_1^{(0)}|^2\lambda^2 + \mathcal{O}\left(\lambda^4\right) = 1. \tag{4.37}$$

When performing the expansion we assume that the other modes only contribute to higher order, $s_i(0) = 0 + \mathcal{O}(\lambda^2)$ for $i \geq 2$, because the second order terms in $\mathbf{s}^\dagger(0)\mathbf{s}(0)$ have to be accurate in the subspace $\mathcal{K}_2$. The condition can then only be fulfilled for any λ when $|s_0^{(0)}|^2 = 1$ and $2\mathrm{Re}[s_0^{(0)}s_0^{(2)}] = -|s_1^{(1)}|^2$. The series expansion as a whole is optimized by first maximizing the zeroth order term, then maximizing the second order term and so on. Because the condition has to be fulfilled for the zeroth order term, the retrieval efficiency is optimized by maximizing the second order term. We can then set $s_0^{(0)} = 1$, which simplifies the second condition to $2\mathrm{Re}[s_0^{(2)}] = -|s_1^{(1)}|^2$, meaning that we only have to maximize with respect to $s_1^{(1)}$. The lowest order

contribution of the optimal spin wave to retrieve from besides $s_0^{(0)} = 1$ is given by

$$\begin{aligned}
\mathrm{Re}s_1^{(1)} =& -\mathrm{Re}\left[\frac{k_{01}^{(1)}\left(k_{00}^{(0)^*}+k_{11}^{(0)}-2\mathrm{Re}k_{00}^{(0)}\right)}{\left(k_{00}^{(0)^*}+k_{11}^{(0)}\right)\left(k_{11}^{(0)}-k_{00}^{(0)}\right)}\right] \\
\mathrm{Im}s_1^{(1)} =& \mathrm{Im}\left[\frac{k_{01}^{(1)}\left(k_{00}^{(0)^*}+k_{11}^{(0)}-2\mathrm{Re}k_{00}^{(0)}\right)}{\left(k_{00}^{(0)^*}+k_{11}^{(0)}\right)\left(k_{11}^{(0)}-k_{00}^{(0)}\right)}\right].
\end{aligned} \tag{4.38}$$

In some cases the optimal spin wave is therefore going to have a nonzero imaginary part. This is important to note, because when applying the time-reversal argument, we assume that we store the light mode in $S(0)$ and retrieve from $S(0)^*$. For a spin wave with nonzero imaginary part, the control pulse then has to be adjusted such that we in the model store and retrieve from the same spin wave. Inserting this optimal spin wave into Eq. (4.36) gives us the maximal retrieval efficiency, which is found to be

$$\begin{aligned}
\eta_r =& \frac{a^{(0)}}{2\mathrm{Re}k_{00}^{(0)}} + \frac{a^{(2)}}{2\mathrm{Re}k_{00}^{(0)}}\lambda^2 - \frac{a^{(0)}\mathrm{Re}k_{00}^{(2)}}{2\left(\mathrm{Re}k_{00}^{(0)}\right)^2}\lambda^2 \\
&+ \frac{a^{(0)}}{2\mathrm{Re}k_{00}^{(0)}}\left|\frac{k_{01}^{(1)}\left(k_{00}^{(0)^*}+k_{11}^{(0)}-2\mathrm{Re}k_{00}^{(0)}\right)}{\left(k_{00}^{(0)^*}+k_{11}^{(0)}\right)\left(k_{11}^{(0)}-k_{00}^{(0)}\right)}\right|^2\lambda^2 \\
&+ 2a^{(0)}\mathrm{Re}\left[\frac{k_{01}^{(1)}k_{10}^{(1)}}{\left(k_{11}^{(0)}-k_{00}^{(0)}\right)^2}\left(\frac{1}{k_{00}^{(0)^*}+k_{11}^{(0)}}+\frac{k_{11}^{(0)}-k_{00}^{(0)}}{4\left(\mathrm{Re}k_{00}^{(0)}\right)^2}-\frac{1}{2\mathrm{Re}k_{00}^{(0)}}\right)\right]\lambda^2 \\
&+ \mathcal{O}\left(\lambda^4\right).
\end{aligned} \tag{4.39}$$

It can now be shown that the zeroth order term indeed is equal to $C/(1+C)$. In order to get a better sense of the second order term, we can look at specific distributions for $\{g^{(i)}\}$, $\{\Omega^{(i)}\}$ and $\{\Delta^{(i)}\}$.

4.2 Inhomogenous Rabi oscillations $\Omega^{(i)}$ and coupling constants $g^{(i)}$

In this section, we will look specifically at the efficiencies for media, which has inhomogeneities with Gaussian distributions of $\{\Omega^{(i)}\}$ and $\{g^{(i)}\}$, but is homogeneously broadened. We limit our calculations to the case where the Λ energy scheme only consists of one excited state. Two different ways to store the incoming quantum field are going to be considered. First, we look at retrieval from a symmetric spin wave mode. This is especially relevant for systems involving storage and retrieval with optical microwaves. Another option, more useful to most other systems, is to retrieve from the spin wave resulting in the highest retrieval efficiency. However, as we will show, this requires making retrieval from a complex spin wave for an off-resonance control beam, which can complicate the application of the time reversal argument for the whole storage-retrieval process.

Inhomogeneous Rabi oscillations and coupling constants can exist in both atomic-vapour and solid-state quantum memories. For both types it is often the case that the interaction strength between the light field and the medium varies in the interaction region. Furthermore, the imperfections in solid-state media lead to inhomogeneous Rabi oscillations and coupling constants. However, this is typically also accompanied by inhomogeneous broadening.

4.2.1 Retrieval efficiency for $\mathcal{K}_2$ subspace

If we look specifically at media with only one excited state and inhomogeneities in $\{\Omega^{(i)}\}$ and $\{g^{(i)}\}$, it allows us to use the general formulation in the last section and make some additional simplifications. The values for $\{\Omega^{(i)}\}$ and $\{g^{(i)}\}$ correspond to a sample drawn from the continuous, Gaussian population. We are interested in finding the expectation value of the retrieval efficiency $\langle \eta_r \rangle_{\text{realization}}$, which is the average for many observations of the retrieval efficiency η_r, which depends on a single sample.

The continuous variable probability density function for Gaussian populations of $\{\Omega^{(i)}\}$ and $\{g^{(i)}\}$ with correlations between them taken into account is

$$\begin{aligned} f(\Omega, g) =& \frac{1}{2\pi\sigma_\Omega\sigma_g\sqrt{1-\rho^2}} \exp\left\{-\frac{1}{2\left(1-\rho^2\right)}\right. \\ & \left.\times\left[\frac{\left(\Omega-\mu_\Omega\right)^2}{\sigma_\Omega^2}+\frac{\left(g-\mu_g\right)^2}{\sigma_g^2}-\frac{2\rho\left(\Omega-\mu_\Omega\right)\left(g-\mu_g\right)}{\sigma_\Omega\sigma_g}\right]\right\} \end{aligned} \tag{4.40}$$

where μ_Ω, μ_g are the population mean values and σ_Ω, σ_g are the population standard deviations. Furthermore, we here have introduced the Pearson product-moment correlation coefficient defined by

$$\rho = \operatorname{cov}(\Omega, g)/(\sigma_\Omega\sigma_g). \tag{4.41}$$

The correlation coefficient has the maximum value $\rho = 1$ for total linear correlation between $\{\Omega^{(i)}\}$ and $\{g^{(i)}\}$ and the minimum value $\rho = -1$ for total negative linear correlation. At $\rho = 0$ there are no correlations between the two distributions.

In the limit where the ensemble consist of a very large number of atoms, the variance of the sample variances $\operatorname{Var}\left(\sum_i \delta{\Omega^{(i)}}^2\right)$, $\operatorname{Var}\left(\sum_i \delta{g^{(i)}}^2\right)$ is going to zero [38]. This means that the sample variance for each sample in this limit is going to be equal to the expectation value of the sample variance

$$\sum_i \delta{\Omega^{(i)}}^2 \to \left\langle \sum_i \delta{\Omega^{(i)}}^2 \right\rangle_{\text{realization}} \quad \text{and} \quad \sum_i \delta{g^{(i)}}^2 \to \left\langle \sum_i \delta{g^{(i)}}^2 \right\rangle_{\text{realization}}$$

for very large N. Because only the dependence of higher order raw moments on the variance contributes to second order in λ, we are also going to make the assumption that all sample raw moments are going to be equal to expectation value of the sample raw moments.

$$\langle \Omega^a g^b \rangle \to \left\langle \langle \Omega^a g^b \rangle \right\rangle_{\text{realization}}$$

Because the expectation value of the sample raw moments is equal to the population raw moments, it is thus possible to use the population probability density function to calculate all the necessary moments when deriving the retrieval efficiency.

$$\langle \Omega^a g^b \rangle = \frac{1}{N}\sum_{i=1}^{N} \Omega^{(i)} g^{(i)} \approx \left\langle \langle \Omega^a g^b \rangle \right\rangle_{\text{realization}} = \int_{-\infty}^{\infty} \Omega^a g^b f(\Omega, g) d\Omega dg \quad \text{for} \quad N \gg 1 \tag{4.42}$$

Furthermore we assume that the exponential tail of the density function is negligible for negative values, since negative $\Omega^{(i)}$ and $g^{(i)}$ do not exist. To fully account for quenched disorder away from this limit, where the samples are relatively small, we would have to calculate

$$\langle \eta_r \rangle_{\text{realization}} = \int \eta_r \left(\{\Omega^{(i)}\}, \{g^{(i)}\} \right) \prod_i f(\Omega_i, g_i) d\Omega_i dg_i. \tag{4.43}$$

Many experiments do however operate with very large ensembles such as quantum memories based on NV-centres.

In this approximation, we can expand the coefficient matrix and the retrieval efficiency in terms of the standard deviations σ_Ω and σ_g, such that we can use the results of the last section. However, because we assume $\{\Delta^{(i)}\}$ to be homogeneous it is possible to define more simple basis vectors compared to the more general case in Eq. (4.20) and (4.21). We will therefore redefine a in Eq. (4.16) such that we now use

$$\mathcal{E}_{\text{out}}(t) = \frac{a}{|a|}\sqrt{\mathbf{v}^\dagger \mathbf{v}} s_0(t) \quad \text{with} \quad a = \frac{\kappa}{\kappa(\gamma + i\Delta) + N\langle g^2 \rangle}. \tag{4.44}$$

The first basis vector is then simply

$$\mathbf{e}_0^\dagger = \frac{\mathbf{g}^T \mathbf{\Omega}}{\sqrt{N\langle g^2 \Omega^2 \rangle}}. \tag{4.45}$$

It is in general more convenient to define a real basis $\mathbf{e}_0$ and $\mathbf{e}_1$, among other things because a complex spin wave $\mathbf{s}(t)$ would transform to complex modes $s_0(t)$, $s_1(t)$ and a real spin wave would transform to real modes. Looking back at Eq. (4.8) we see that the basis vector $\mathbf{e}_1$ is defined through

$$\mathbf{e}_0^\dagger \mathbf{A} \left(1 - \mathbf{e}_0 \mathbf{e}_0^\dagger \right) = k_{01} \mathbf{e}_1^\dagger \quad \text{and} \quad \mathbf{e}_1^\dagger \mathbf{e}_1 = 1. \tag{4.46}$$

In the more general case we defined k_{01} to be real with complex $\mathbf{e}_1$. However, for homogeneous $\{\Delta^{(i)}\}$ we can define a real vector $\mathbf{e}_1$ and absorb the complex part into k_{01}. The real second basis vector is then

$$\mathbf{e}_1^\dagger = \frac{\langle g^2 \Omega^2 \rangle \mathbf{g}^T \mathbf{\Omega}^3 - \langle g^2 \Omega^4 \rangle \mathbf{g}^T \mathbf{\Omega}}{\sqrt{N}\left(\langle g^2 \Omega^2 \rangle^2 \langle g^2 \Omega^6 \rangle - \langle g^2 \Omega^2 \rangle \langle g^2 \Omega^4 \rangle^2 \right)^{1/2}}. \tag{4.47}$$

Having found the first two basis vectors and defined the moments allows us to expand the elements of the coefficient matrix $k_{ij} = \mathbf{e}_i^\dagger \mathbf{A} \mathbf{e}_j$ in terms of the standard deviation such that

$$k_{ij} = k_{ij}^{(0)} + k_{ij}^{(2)}\lambda^2 + \mathcal{O}\left(\lambda^4\right) = k_{ij}^{(00)} + k_{ij}^{(11)}\sigma_g\sigma_\Omega + k_{ij}^{(20)}\sigma_g^2 + k_{ij}^{(02)}\sigma_\Omega^2 + \mathcal{O}\left(\lambda^4\right). \tag{4.48}$$

The series expansions of the elements of the coefficient matrix needed to calculate the efficiency up to second order in λ are:

$$\begin{aligned}
k_{00} =& \frac{1}{\gamma + i\Delta}\left(\frac{\left\langle g^2\Omega^4\right\rangle}{\left\langle g^2\Omega^2\right\rangle} - \frac{N\left\langle g^2\Omega^2\right\rangle}{\kappa\left(\gamma+i\Delta\right)+N\left\langle g^2\right\rangle}\right) \\
=& \frac{\mu_\Omega^2}{\gamma}\frac{1}{1+i\frac{\Delta}{\gamma}+C} + \frac{4\mu_\Omega}{\mu_g\gamma}\frac{1}{1+i\frac{\Delta}{\gamma}+C}\rho\sigma_g\sigma_\Omega - \frac{N\mu_\Omega^2}{\gamma^2\kappa}\frac{1}{\left(1+i\frac{\Delta}{\gamma}+C\right)^2}\sigma_g^2 \\
&+ \left(\frac{5}{\gamma}\frac{1}{1+i\frac{\Delta}{\gamma}} - \frac{1}{\gamma}\frac{1}{1+i\frac{\Delta}{\gamma}}\frac{C}{1+i\frac{\Delta}{\gamma}+C}\right)\sigma_\Omega^2 + \mathcal{O}\left(\lambda^4\right) \qquad (4.49)\\
k_{01} =& k_{10} = \frac{1}{\gamma+i\Delta}\left(\frac{\left\langle g^2\Omega^6\right\rangle}{\left\langle g^2\Omega^2\right\rangle} - \frac{\left\langle g^2\Omega^4\right\rangle^2}{\left\langle g^2\Omega^2\right\rangle^2}\right)^{1/2} \\
=& \frac{2\mu_\Omega}{\gamma+i\Delta}\sigma_\Omega + \mathcal{O}\left(\lambda^3\right) \qquad (4.50)\\
k_{11} =& \frac{1}{\gamma+i\Delta}\frac{\left\langle g^2\Omega^2\right\rangle^2\left\langle g^2\Omega^8\right\rangle - 2\left\langle g^2\Omega^2\right\rangle\left\langle g^2\Omega^4\right\rangle\left\langle g^2\Omega^6\right\rangle + \left\langle g^2\Omega^4\right\rangle^3}{\left\langle g^2\Omega^2\right\rangle^2\left\langle g^2\Omega^6\right\rangle - \left\langle g^2\Omega^2\right\rangle\left\langle g^2\Omega^4\right\rangle^2} \\
=& \frac{\mu_\Omega^2}{\gamma+i\Delta} + \mathcal{O}\left(\lambda^2\right) \qquad (4.51)
\end{aligned}$$

Here k_{00} and k_{11} are just a simplification of the more general case in the previous section. However, because we have defined a real $\mathbf{e}_1$, the definition of k_{01} and k_{10} is slightly different. The elements in the coefficient matrix define the time dependence of the outgoing quantum field $\mathcal{E}_{\text{out}}(t) = \frac{a}{|a|}\sqrt{\mathbf{v}^\dagger\mathbf{v}}s_0(t)$ such that we now can approximate the mode $s_0(t)$. In order to determine the right normalization we also find

$$\begin{aligned}
\mathbf{v}^\dagger\mathbf{v} =& \frac{2N\left\langle g^2\Omega^2\right\rangle}{\kappa\left(\gamma^2+\Delta^2\right)}\left|\frac{\kappa\left(\gamma+i\Delta\right)}{\kappa\left(\gamma+i\Delta\right)+N\left\langle g^2\right\rangle}\right|^2 \\
=& \frac{2\mu_g^2\mu_\Omega^2}{\gamma}\frac{C}{\left(1+C\right)^2+\frac{\Delta^2}{\gamma^2}} + \frac{8\mu_g\mu_\Omega}{\gamma}\frac{C}{\left(1+C\right)^2+\frac{\Delta^2}{\gamma^2}}\rho\sigma_g\sigma_\Omega \\
&+ \frac{2N\mu_\Omega^2}{\gamma^2\kappa}\frac{1+\frac{\Delta^2}{\gamma^2}-\frac{N^2\mu_g^2}{\kappa^2\gamma^2}}{\left[\left(1+C\right)^2+\frac{\Delta^2}{\gamma^2}\right]^2}\sigma_g^2 + \frac{2\mu_g^2}{\gamma}\frac{C}{\left(1+C\right)^2+\frac{\Delta^2}{\gamma^2}}\sigma_\Omega^2 + \mathcal{O}\left(\lambda^4\right). \qquad (4.52)
\end{aligned}$$

Besides from $\mathbf{v}^\dagger\mathbf{v}$ and the coefficient matrix, the retrieval efficiency only depends on the initial spin wave before readout.

4.2.2 Retrieval from symmetric spin wave

We will now look at retrieval from a spin wave where all excitations are stored evenly among all atoms. This symmetric spin wave is real and has the form $\mathbf{s}(0) = \{1,1,\ldots,1\}/\sqrt{N}$. As shown in section 2.4, retrieval from the symmetric spin wave leads to the maximal retrieval efficiency for systems with homogeneous $\{g^{(i)}\}$, $\{\Omega^{(i)}\}$

and $\{\Delta^{(i)}\}$. Storage and retrieval from this type of spin wave is relevant for experiments, where microwave photons are coupled to the atomic ensemble [39, 40]. Because of the large wavelength, the light does in this case not interact very strongly with the inhomogeneities and mainly couples to the symmetric mode.

The retrieval efficiency can be found from the general formula in Eq. (4.36) for any type of initial spin wave. In order to use the equation, we have to find how the individual atomic excitations are transformed into the collective modes $s_0(0) = \mathbf{e}_0^\dagger \mathbf{s}(0)$ and $s_1(0) = \mathbf{e}_1^\dagger \mathbf{s}(0)$. Using the previously defined basis vectors, we get that the spin wave transforms into the modes

$$s_0(0) = 1 - \frac{1}{2}\frac{\sigma_g^2}{\mu_g^2} - \frac{1}{2}\frac{\sigma_\Omega^2}{\mu_\Omega^2} - \rho\frac{\sigma_g}{\mu_g}\frac{\sigma_\Omega}{\mu_\Omega} + \mathcal{O}\left(\lambda^4\right) \tag{4.53}$$

$$s_1(0) = -\rho\frac{\sigma_g}{\mu_g} - \frac{\sigma_\Omega}{\mu_\Omega} + \mathcal{O}\left(\lambda^3\right). \tag{4.54}$$

The retrieval efficiency from Eq. (4.36) is then

$$\begin{aligned}\eta_r =& \frac{C}{1+C} - \frac{C}{1+C}\left[1 + \frac{\Delta^2}{\gamma^2}\frac{4}{(1+C)(2+C)}\right]\frac{\sigma_\Omega^2}{\mu_\Omega^2} - \frac{C^2}{(1+C)^2}\frac{\sigma_g^2}{\mu_g^2} \\ &+ \frac{2C^2\rho}{(1+C)(2+C)}\frac{\sigma_\Omega}{\mu_\Omega}\frac{\sigma_g}{\mu_g} + \mathcal{O}\left(\lambda^4\right).\end{aligned} \tag{4.55}$$

In Figure 4.39 the symbolic solution for the retrieval efficiency is plotted as a function of standard deviation for various parameters together with the numerical solutions, as described in section 3.2. The data points of the numerical solution are averages of ten calculations with random picks for a sample of $N = 200$ atoms. When we compare the symbolic solution with the numerical solution, we observe that there is agreement to second order, even for this relatively small ensemble. However, higher order terms not accounted for in the symbolic solution become significant for high standard deviation in (a) and (b). The results in the figure show that inhomogeneities in the ensemble tend to decrease the retrieval efficiency. In (a) higher correlations between $\left\{\Omega^{(i)}\right\}$ and $\left\{g^{(i)}\right\}$ lead to a higher retrieval efficiency and in (b) lower detuning lead to a higher retrieval efficiency. Changing γ in (c) and changing κ in (d) lead to very similar results, because both these variations mainly change the value of $C = N\mu_g^2/(\kappa\gamma)$. We note, that all of these important observations can be made by solely analyzing the symbolic solution up to second order.

4.2.3 Optimal retrieval

Retrieval from the symmetric spin wave leads only to the maximal retrieval efficiency for a homogeneous ensemble. For light below microwave wavelength it is therefore more relevant to map to a spin wave with higher efficiency. By using Eq. (4.39) we can find the maximal retrieval efficiency when retrieving from a different spin wave

$$\eta_r = \frac{C}{1+C} - \frac{4C}{1+C}\left[\frac{1+C}{(2+C)^2} + \frac{\Delta^2}{\gamma^2}\frac{1}{(1+C)(2+C)^2}\right]\frac{\sigma_\Omega^2}{\mu_\Omega^2} + \frac{C}{(1+C)^2}\frac{\sigma_g^2}{\mu_g^2} + \mathcal{O}\left(\lambda^4\right). \tag{4.56}$$

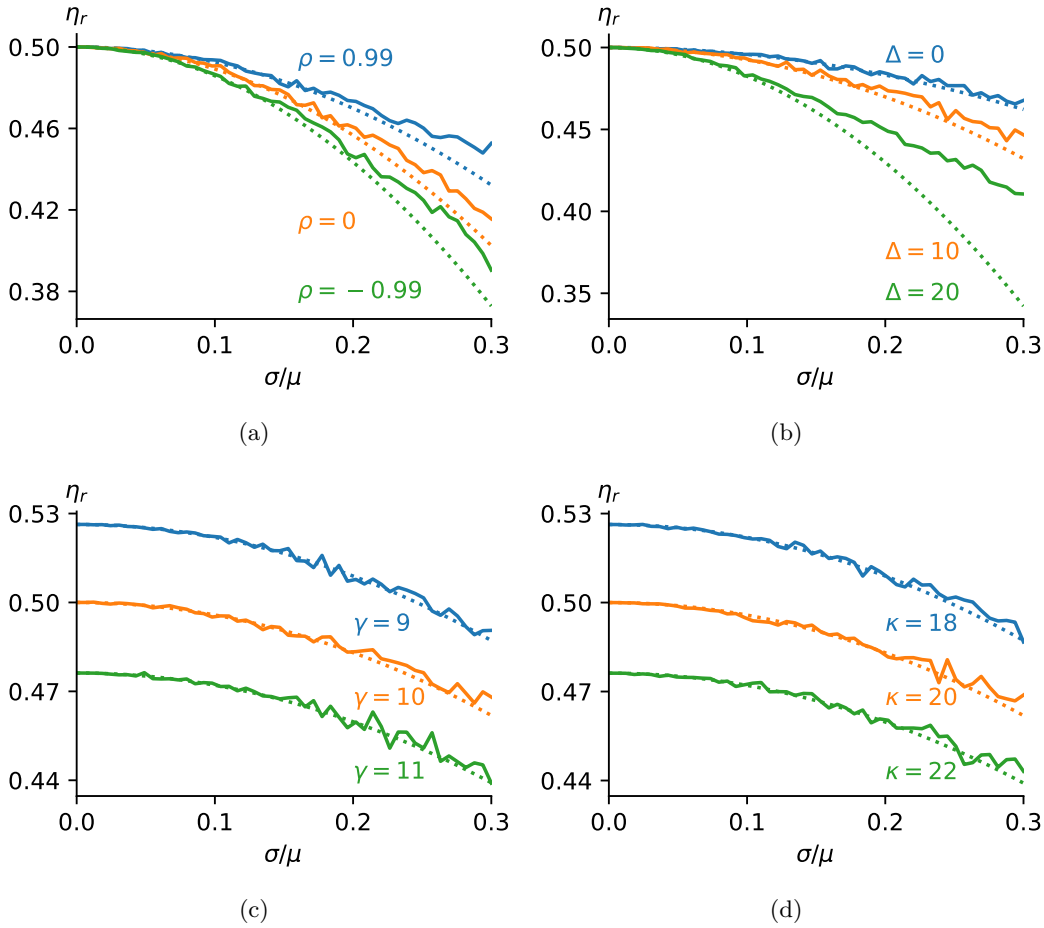

Figure 4.1: Retrieval efficiency η_r as a function of $\sigma/\mu = \sigma_\Omega/\mu_\Omega = \sigma_g/\mu_g$ for retrieval from the symmetric spin wave mode. The numerical (solid) and the approximate symbolic (dotted) solutions are in good agreement up to second order in σ/μ. In order to smooth out variation in the numerical solutions, the data points of the numerical solution are averages of ten calculations with $N = 200$ random samples drawn from a Gaussian distribution. The following values, except when other values are displayed beside the lines, have been used in the calculations: $\rho = 0.99$, $\Delta = 1$, $\gamma = 10$, $\kappa = 20$, $\mu_g = 1$, $\mu_\Omega = 10$. Therefore $C = 1$ in (a) and (b) and is varied in (c) and (d).

We note that the equation is independent of the correlation coefficient ρ up to second order in σ_Ω and σ_g. The second order term would therefore remain unchanged, if we would assume that the moments could be separated such that $\langle \Omega^a g^b \rangle = \langle \Omega^a \rangle \langle g^b \rangle$, which is the case for no correlations $\rho = 0$. This means that the terms independent of σ_Ω^2 are in agreement with the result in section 2.4 and Eq. (2.16). Introducing new collective variables for homogeneous $\{\Omega^{(i)}\}$ allowed us here to solve the dynamics accurately with $\eta_r = \tilde{C}/(1+\tilde{C})$ and $\tilde{C} = \sum_i {g^{(i)}}^2/(\kappa\gamma)$. The second order expansion in σ_g of $\tilde{C}/(1+\tilde{C})$ is then $C/[(1+C)^2\mu_g]$ as in Eq. (4.56).

In Figure 4.39 the symbolic solution for the retrieval efficiency is plotted together with the numerical solution. Compared to retrieval from the symmetric mode we obtain higher efficiencies, but apart from that, the behavior is very similar. The symbolic solution is in agreement with the numerical solution up to second order and inhomogeneities in $\left\{\Omega^{(i)}\right\}$ still lead to a decrease in efficiency. Correlations ρ affect the efficiency to higher order as seen in (a) with correlated distributions being most efficient. In (c) and (d) we see that higher C leads to a higher retrieval efficiency. A very important result is that using a laser with small detuning is more efficient than using large detuning. Again this is the same observation as for the symmetric mode. This is in contrast to other work [41], were it has been suggested that working in the far-detuned regime is preferable.

In order to find the spin wave from which retrieval is most efficient, we use Eq. (4.38) to calculate the first order term of the initial mode $s_1(0)$. Because $k_{01} = k_{10} = 2\mu_\Omega/(\gamma + i\Delta)\sigma_\Omega + \mathcal{O}(\lambda^3)$ only has a first order expansion in σ_Ω, implies that the optimal mode $s_1(0)$ only has a first order expansion in σ_Ω when applying Eq. (4.38).

$$s_1^{(1)}(0)\lambda = -2\frac{1+C}{2+C}\frac{\sigma_\Omega}{\mu_\Omega} - i\frac{\Delta}{\gamma}\frac{2}{2+C}\frac{\sigma_\Omega}{\mu_\Omega}. \tag{4.57}$$

When deriving Eq. (4.38) we already have assumed that $s_0^{(0)} = 1$ and $2\mathrm{Re}[s_0^2] = -|s_1^{(1)}|^2$. All other spin wave modes are higher order. The outcome for $s_1^{(1)}$ is consistent with the results in section 2.4, where we only looked at inhomogeneities in $\{g^{(i)}\}$. For $\sigma_\Omega = 0$ the optimal spin wave mode to retrieve from is $s_0(0) = 1$ with all other initial modes being zero. Since $s_i(0) = \mathbf{e}_i^\dagger \mathbf{s}(0)$ this means that the optimal spin wave is $\mathbf{s}(0) = \mathbf{e}_0$, where $\mathbf{e}_0$ is as defined in Eq. (4.45) with no inhomogeneities in $\{\Omega^{(i)}\}$. Looking back at Eq. (2.14), this is indeed corresponds to using the collective variable for s in section 2.4.

Furthermore we notice that the spin wave onto which we have to store in order the achieve the highest possible retrieval efficiency has an imaginary part, when the control beam is off-resonance. Because the mode $s_1(0)$ has an imaginary part, we also know that the initial spin wave $\mathbf{s}(0)$ has an imaginary part. This means that we have to be careful about applying the time-reverse argument for experiments with off-resonant control beam. Simply applying the time-reverse argument would mean that we would assume that we retrieve from $\mathbf{s}$, but are actually storing the light in $\mathbf{s}^*$ (see chapter 5).

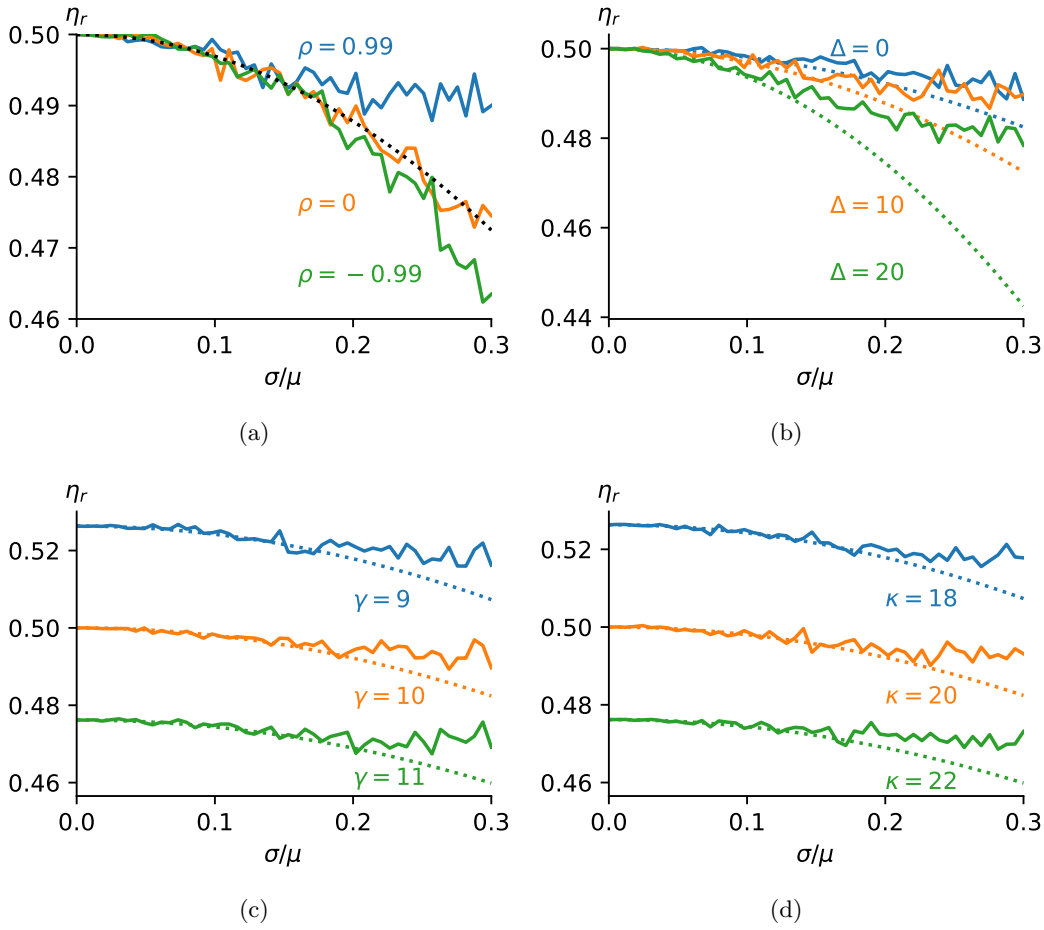

Figure 4.2: Retrieval efficiency η_r as a function of $\sigma/\mu = \sigma_\Omega/\mu_\Omega = \sigma_g/\mu_g$ for retrieval from the optimal spin wave mode. The numerical (solid) and the approximate symbolic (dotted) solutions are in good agreement up to second order in σ/μ. In order to smooth out variation in the numerical solutions, the data points of the numerical solution are averages of ten calculations with $N = 200$ random samples drawn from a Gaussian distribution. The following values, except when other values are displayed beside the lines, have been used in the calculations: $\rho = 0.99$, $\Delta = 1$, $\gamma = 10$, $\kappa = 20$, $\mu_g = 1$, $\mu_\Omega = 10$. Therefore $C = 1$ in (a) and (b) and is varied in (c) and (d).

4.3 Inhomogeneous broadening

We will now look specifically at how the maximum retrieval efficiency is related to inhomogeneous broadened media with a Gaussian population distribution of $\{\Delta^{(i)}\}$, but homogeneous Rabi oscillations $\{\Omega^{(i)}\}$ and coupling constant $\{g^{(i)}\}$. Again we restrict the model to the case where the Λ energy scheme only has one excited level. Furthermore the initial spin wave which facilitates maximal retrieval is analyzed.

In order to determine the maximal retrieval efficiency from the definition in section 4.1.2, we have find the series expansion of the elements $k_{00}, k_{10}, k_{01}, k_{11}$ of the coefficient matrix and the series expansion of $\mathbf{v}^\dagger\mathbf{v}$. Contrary to the derivations in section 4.2 we cannot define real orthonormal basis vectors of the coefficient matrix, because the imaginary part of $\mathbf{v}$ depends on the inhomogeneous distribution. Therefore, we find the first two basis vectors directly from Eq. (4.20) and Eq. (4.21), where we just assume $\left\{\Omega^{(i)}\right\}$ and $\left\{g^{(i)}\right\}$ to be homogeneous and real.

$$\mathbf{e}_0^\dagger = \frac{\mathbf{1}^T\tilde{\mathbf{\Delta}}^{-1}}{\sqrt{N\left\langle|\tilde{\Delta}|^{-2}\right\rangle}} \tag{4.58}$$

$$\mathbf{e}_1^\dagger = \frac{\left\langle|\tilde{\Delta}|^{-2}\right\rangle\mathbf{1}^T\left(\tilde{\mathbf{\Delta}}^{-1}\right)^2 - \left\langle|\tilde{\Delta}|^{-2}\tilde{\Delta}^{-1}\right\rangle\mathbf{1}^T\tilde{\mathbf{\Delta}}^{-1}}{\sqrt{N}\left(\left\langle|\tilde{\Delta}|^{-2}\right\rangle^2\left\langle|\tilde{\Delta}|^{-4}\right\rangle - \left\langle|\tilde{\Delta}|^{-2}\right\rangle\left|\left\langle|\tilde{\Delta}|^{-2}\tilde{\Delta}^{-1}\right\rangle\right|^2\right)^{1/2}} \tag{4.59}$$

$$\mathbf{1}^T = \begin{pmatrix}1 & 1 & 1 & \dots & 1\end{pmatrix} \tag{4.60}$$

Again we calculate the moments of the discrete sample distribution by using the probability density function of a continuous Gaussian distribution, which we can assume to be valid for very large N.

$$\langle\tilde{\Delta}^{-a}\rangle = \frac{1}{N}\sum_{i=1}^{N}\frac{1}{\gamma+i\Delta^{(i)}} \approx \left\langle\langle\tilde{\Delta}^{-a}\rangle\right\rangle_{\text{realization}} = \int_{-\infty}^{\infty}\frac{1}{(\gamma+i\Delta)^a}f(\Delta)d\Delta \quad \text{for} \quad N \gg 1 \tag{4.61}$$

In this equation denotes $f(\Delta)$ the probability density function of a Gaussian distribution with mean μ_Δ and standard deviation σ_Δ.

$$f(\Delta) = \frac{1}{2\pi\sigma_\Delta}\exp\left(-\frac{(\Delta-\mu_\Delta)^2}{2\sigma_\Delta^2}\right) \tag{4.62}$$

Having described how the moments are calculated and defined the first two basis vectors allows us to find the expansion of the coefficient matrix directly from the more general definitions in Eq. (4.22) - (4.24) or through $k_{ij} = \mathbf{e}_i^\dagger\mathbf{A}\mathbf{e}_j$. Furthermore we find the series expansion of $\mathbf{v}^\dagger\mathbf{v}$.

$$
\begin{aligned}
k_{00} =& \Omega^2 \left(\frac{\left\langle |\tilde{\Delta}|^{-2} \tilde{\Delta}^{-1} \right\rangle}{\left\langle |\tilde{\Delta}|^{-2} \right\rangle} - \frac{N \left\langle \tilde{\Delta}^{-2} \right\rangle}{\kappa + N g^2 \left\langle \tilde{\Delta}^{-1} \right\rangle} \right) \\
=& \frac{\Omega^2}{\gamma} \frac{1}{1 + C + i\frac{\mu_\Delta}{\gamma}} + \frac{\Omega^2}{\gamma^3} \frac{C - 1 + C^2 + 2i\frac{\mu_\Delta}{\gamma} + 3iC\frac{\mu_\Delta}{\gamma} - 3\frac{\mu_\Delta^2}{\gamma^2}}{\left(1 + \frac{\mu_\Delta^2}{\gamma^2}\right)\left(1 + i\frac{\mu_\Delta}{\gamma}\right)\left(1 + C + i\frac{\mu_\Delta}{\gamma}\right)^2} \sigma_\Delta^2 + \mathcal{O}\left(\sigma_\Delta^4\right)
\end{aligned} \tag{4.63}
$$

$$
\begin{aligned}
k_{01} =& \Omega^2 \left(\frac{\left\langle |\tilde{\Delta}|^{-4} \right\rangle}{\left\langle |\tilde{\Delta}|^{-2} \right\rangle} - \frac{\left| \left\langle |\tilde{\Delta}|^{-2} \tilde{\Delta}^{-1} \right\rangle \right|^2}{\left\langle |\tilde{\Delta}|^{-2} \right\rangle^2} \right)^{1/2} \\
=& \frac{\Omega^2}{\gamma^2} \frac{1}{\left(1 + \frac{\mu_\Delta^2}{\gamma^2}\right)} \sigma_\Delta + \mathcal{O}\left(\sigma_\Delta^3\right)
\end{aligned} \tag{4.64}
$$

$$
\begin{aligned}
k_{10} =& \Omega^2 \left(\left\langle |\tilde{\Delta}|^{-2} \right\rangle^3 \left\langle |\tilde{\Delta}|^{-4} \right\rangle - \left\langle |\tilde{\Delta}|^{-2} \right\rangle^2 \left| \left\langle |\tilde{\Delta}|^{-2} \tilde{\Delta}^{-1} \right\rangle \right|^2 \right)^{-1/2} \\
& \times \left[\left\langle |\tilde{\Delta}|^{-2} \right\rangle \left\langle |\tilde{\Delta}|^{-2} \tilde{\Delta}^{-2} \right\rangle - \left\langle |\tilde{\Delta}|^{-2} \tilde{\Delta}^{-1} \right\rangle^2 \right. \\
& \left. + N \frac{\left\langle |\tilde{\Delta}|^{-2} \tilde{\Delta}^{-1} \right\rangle \left\langle |\tilde{\Delta}|^{-2} \right\rangle \left\langle \tilde{\Delta}^{-2} \right\rangle - \left\langle |\tilde{\Delta}|^{-2} \right\rangle^2 \left\langle \tilde{\Delta}^{-3} \right\rangle}{\kappa + N g^2 \left\langle \tilde{\Delta}^{-1} \right\rangle} \right] \\
=& \frac{\Omega^2}{\gamma^2} \frac{-1 + C + i\frac{\mu_\Delta}{\gamma}}{\left(1 + i\frac{\mu_\Delta}{\gamma}\right)^2 \left(1 + C + i\frac{\mu_\Delta}{\gamma}\right)} \sigma_\Delta + \mathcal{O}\left(\sigma_\Delta^3\right)
\end{aligned} \tag{4.65}
$$

$$
\begin{aligned}
k_{11} =& \Omega^2 \left(\left\langle |\tilde{\Delta}|^{-2} \right\rangle^2 \left\langle |\tilde{\Delta}|^{-4} \right\rangle - \left\langle |\tilde{\Delta}|^{-2} \right\rangle \left| \left\langle |\tilde{\Delta}|^{-2} \tilde{\Delta}^{-1} \right\rangle \right|^2 \right)^{-1} \\
& \times \left[\left\langle |\tilde{\Delta}|^{-2} \right\rangle^2 \left\langle |\tilde{\Delta}|^{-4} \tilde{\Delta}^{-1} \right\rangle - \left\langle |\tilde{\Delta}|^{-2} \right\rangle \left\langle |\tilde{\Delta}|^{-2} \tilde{\Delta}^{*-1} \right\rangle \left\langle |\tilde{\Delta}|^{-2} \tilde{\Delta}^{-2} \right\rangle \right. \\
& \left. - \left\langle |\tilde{\Delta}|^{-2} \right\rangle \left\langle |\tilde{\Delta}|^{-2} \tilde{\Delta}^{-1} \right\rangle \left\langle |\tilde{\Delta}|^{-4} \right\rangle + \left| \left\langle |\tilde{\Delta}|^{-2} \tilde{\Delta}^{-1} \right\rangle \right|^2 \left\langle |\tilde{\Delta}|^{-2} \tilde{\Delta}^{-1} \right\rangle \right] \\
=& \frac{\Omega^2}{\gamma} \frac{1}{1 + i\frac{\mu_\Delta}{\gamma}} + \mathcal{O}\left(\sigma_\Delta^2\right)
\end{aligned} \tag{4.66}
$$

$$
\begin{aligned}
\mathbf{v}^\dagger \mathbf{v} =& \frac{2\Omega^2}{\gamma} \frac{C \left\langle |\tilde{\Delta}|^{-2} \right\rangle}{\left| \frac{1}{\gamma} + C \left\langle \tilde{\Delta}^{-1} \right\rangle \right|^2} \\
=& \frac{2C^2\Omega}{\gamma^3} \frac{1}{\left(1 + \frac{\mu_\Delta^2}{\gamma^2}\right)\left[(1 + C)^2 + \frac{\mu_\Delta^2}{\gamma^2}\right]} \\
& - \frac{4C^2\Omega}{\gamma^5} \frac{1 + C - \left(2 + 3C + 2C^2\right)\frac{\mu_\Delta^2}{\gamma^2} - 3\frac{\mu_\Delta^4}{\gamma^4}}{\left(1 + \frac{\mu_\Delta^2}{\gamma^2}\right)^3 \left[(1 + C)^2 + \frac{\mu_\Delta^2}{\gamma^2}\right]^2} \sigma_\Delta^2 + \mathcal{O}\left(\sigma_\Delta^4\right)
\end{aligned} \tag{4.67}
$$

The different terms of the series expansion can then be used to calculate the optimal retrieval efficiency by using Eq. (4.39)

$$\eta_r = \frac{C}{1+C} - \frac{C}{(2+3C+C^2)^2}\frac{\sigma_\Delta^2}{\gamma^2} + \mathcal{O}\left(\sigma_\Delta^4\right). \tag{4.68}$$

Clearly, the result shows that inhomogeneous broadening leads to a decrease in the optimal retrieval efficiency. A very important result is that the retrieval efficiency in this case is independent of the mean detuning and only depends on the standard deviation. Both observations are affirmed in Fig. 4.3, where we compare the symbolic solution with the numerical solution. The behavior in (a) suggest that the maximal retrieval efficiency even is independent of mean detuning to higher order in σ_Δ. An identical conclusion has been reached by Gorshkov et al. in [4], where retrieval from inhomogeneously broadened medium in free space has been analyzed. In both (b) and (c) the behavior is similar to the corresponding figure in the last section. A high retrieval efficiency is obtained for a high cooperativity parameter C.

Having determined the different terms of the series expansions allows us also to find the spin wave which facilitates maximal retrieval by using Eq. (4.38).

$$s_1^{(1)}(0)\lambda = \frac{-1 - \frac{\mu_\Delta^2}{\gamma^2} - C + i\frac{\mu_\Delta}{\gamma}C}{(2+C)\left(1+\frac{\mu_\Delta^2}{\gamma^2}\right)}\frac{\sigma_\Delta}{\gamma} \tag{4.69}$$

In contrast to the previous section, we cannot deduce directly from the shape of the equation if the spin wave is real or complex, because we have used complex basis vectors in the derivation. Therefore, we need to go back at how the spin wave modes have been defined. It is not possible to find the exact spin wave $\mathbf{s}$ from a finite number of modes $\{s_i(t)\}$ and thus not possible to find the real and imaginary part of $\mathbf{s}$. However, because the basis is complex we expect the initial spin wave to be complex for all average detuning.

Because quantum memories with inhomogeneous broadening typically also have inhomogeneous Rabi oscillations and coupling constants, it would be relevant to take all these types of inhomogeneities into account when calculating the retrieval efficiency. This requires new calculations if second order correlations between any of these inhomogeneities affect the maximal retrieval efficiency and they have to be included. When it is not necessary to include these correlations in the model, we can simply try to add the results in Eq. (4.68) and Eq. (4.56).

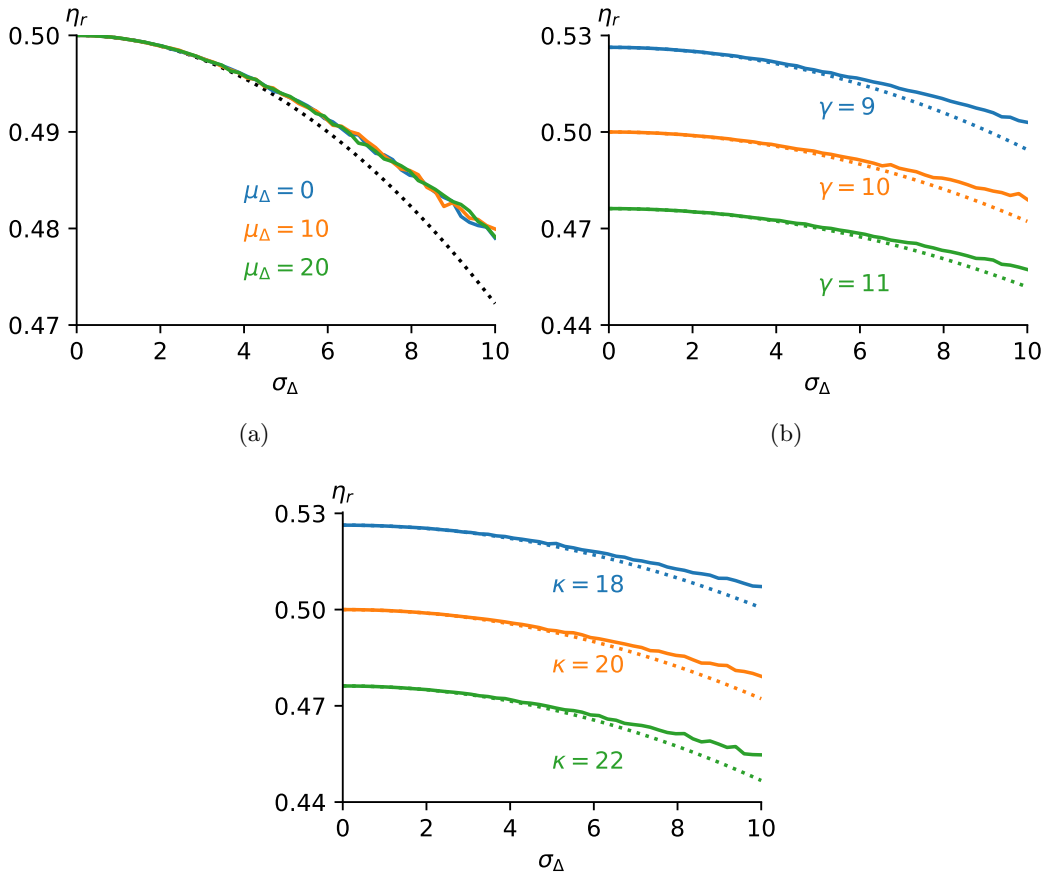

Figure 4.3: Retrieval efficiency η_r as a function of σ_Δ for retrieval from the optimal spin wave mode. The numerical (solid) and the approximate symbolic (dotted) solutions are in good agreement up to second order in σ_Δ. In order to smooth out variation in the numerical solutions, the data points of the numerical solution are averages of ten calculations with $N = 200$ random samples drawn from a Gaussian distribution. The following values, except when other values are displayed beside the lines, have been used in the calculations: $\mu_\Delta = 1$, $\gamma = 10$, $\kappa = 20$, $g = 1$, $\Omega = 10$. Therefore $C = 1$ in (a) and is varied in (b) and (c).

Chapter 5

Optimization of storage and retrieval

The strategy for optimizing the retrieval process with regard to the retrieval efficiency is not necessarily the best strategy for optimizing the retrieval process with regard to the total efficiency taking both storage and retrieval into account. When optimizing with respect to the retrieval efficiency, we could find the optimal spin wave to retrieve from. However, in the case where we look at the whole process, we need to balance the feasibility of the stored spin wave for efficient retrieval with the feasibility for efficient storage. In this chapter, we first analyze under which conditions the strategy for optimizing the retrieval efficiency can be applied for optimizing the total storage-retrieval efficiency. Furthermore we find a numerical method for calculating the maximum storage-retrieval efficiency, before looking specifically at systems with inhomogeneous coupling canstants and Rabi oscillations and systems with inhomogeneous broadening.

In the previous sections we have tried to analyze the retrieval process and developed methods to calculate the retrieval efficiency. These methods can in general not be applied to calculate the storage efficiency, which makes it more difficult to analyze the storage process. In some cases it is however possible to use a strategy where an optimal storage efficiency is obtained, which is identical to the optimal retrieval efficiency. Furthermore the time-reversal argument can be used to find the storage efficiency with the knowledge of the retrieval process. Once it has become more clear how the retrieval process is connected to storage process, it is possible to find optimal strategies for the total process.

5.1 Conditions for optimizing both storage and retrieval

We have previously determined the spin waves, which allow for optimal retrieval. Ideally we are able store the incoming light field with the maximal retrieval efficiency into one of these optimal spin waves, before then being able to perform retrieval with the maximal efficiency. Because both storage and retrieval has been optimized, it is certain that this strategy gives the maximal total efficiency. In the following, we determine the conditions for when this is possible.

For simplicity of notation we are going to use the Schrödinger picture to formalize the mappings during storage and retrieval. The subspace A of the Hilbert space $\mathcal{H}$ contains the spin wave modes and the subspace B contains the photon modes. During storage the linear map $\mathbf{M}$ transforms the incoming light field $|\boldsymbol{\mathcal{E}}_{\text{in}}\rangle \in B$ to the stored spin wave $|\mathbf{s}\rangle \in A$. Similarly during retrieval the linear map $\mathbf{M}'^{\dagger}$ transforms the stored spin wave $|\mathbf{s}\rangle \in A$ to the outgoing light field $|\boldsymbol{\mathcal{E}}_{\text{out}}\rangle \in B$. These transformations are then denoted as

$$|\mathbf{s}\rangle = \mathbf{M}\,|\boldsymbol{\mathcal{E}}_{\text{in}}\rangle \quad \text{and} \quad |\boldsymbol{\mathcal{E}}_{\text{out}}\rangle = \mathbf{M}'^{\dagger}\,|\mathbf{s}\rangle\,. \tag{5.1}$$

Because the maps are linear, it is according to fundamental mathematical theorems possible to use the singular-value decomposition to decompose them such that

$$\mathbf{M} = \sum_k \sqrt{\lambda_s^{(k)}}\left|\mathbf{s}_s^{(k)}\right\rangle\left\langle\boldsymbol{\mathcal{E}}_s^{(k)}\right| \quad \text{and} \quad \mathbf{M}' = \sum_k \sqrt{\lambda_r^{(k)}}\left|\mathbf{s}_r^{(k)}\right\rangle\left\langle\boldsymbol{\mathcal{E}}_r^{(k)}\right| \tag{5.2}$$

where $\sqrt{\lambda_s^{(k)}}, \sqrt{\lambda_r^{(k)}}$ are the singular values and $|\mathbf{s}_s^{(k)}\rangle, |\mathbf{s}_r^{(k)}\rangle \in A$ and $|\boldsymbol{\mathcal{E}}_s^{(k)}\rangle, |\boldsymbol{\mathcal{E}}_r^{(k)}\rangle \in B$ are respectively the orthonormal left-singular and right-singular vectors. The storage and retrieval efficiencies are then in terms of the maps defined as:

$$\eta_s = \frac{\langle\mathbf{s}|\,\mathbf{s}\rangle}{\langle\boldsymbol{\mathcal{E}}_{\text{in}}|\,\boldsymbol{\mathcal{E}}_{\text{in}}\rangle} = \frac{\langle\boldsymbol{\mathcal{E}}_{\text{in}}|\,\mathbf{M}^{\dagger}\mathbf{M}\,|\boldsymbol{\mathcal{E}}_{\text{in}}\rangle}{\langle\boldsymbol{\mathcal{E}}_{\text{in}}|\,\boldsymbol{\mathcal{E}}_{\text{in}}\rangle} = \sum_k \lambda_s^{(k)} \frac{\left|\left\langle\boldsymbol{\mathcal{E}}_s^{(k)}\right|\,\boldsymbol{\mathcal{E}}_{\text{in}}\right\rangle\right|^2}{\langle\boldsymbol{\mathcal{E}}_{\text{in}}|\,\boldsymbol{\mathcal{E}}_{\text{in}}\rangle} \tag{5.3}$$

$$\eta_r = \frac{\langle\boldsymbol{\mathcal{E}}_{\text{out}}|\,\boldsymbol{\mathcal{E}}_{\text{out}}\rangle}{\langle\mathbf{s}|\,\mathbf{s}\rangle} = \frac{\langle\mathbf{s}|\,\mathbf{M}'\mathbf{M}'^{\dagger}\,|\mathbf{s}\rangle}{\langle\mathbf{s}|\,\mathbf{s}\rangle} = \sum_k \lambda_r^{(k)} \frac{\left|\left\langle\mathbf{s}_r^{(k)}\right|\,\mathbf{s}\right\rangle\right|^2}{\langle\mathbf{s}|\,\mathbf{s}\rangle} \tag{5.4}$$

This shows that the efficiencies are determined by the eigenvalues and the overlap of the incoming state with the eigenvectors of the hermitian matrices $\mathbf{M}^{\dagger}\mathbf{M}$ and $\mathbf{M}'\mathbf{M}'^{\dagger}$. Because of the variational principle we know that the maximum eigenvalue of these matrices corresponds to maximum efficiency during storage and retrieval such that

$$\eta_s^{\max} = \max\left\{\lambda_s^{(k)}\right\} \quad \text{and} \quad \eta_r^{\max} = \max\left\{\lambda_r^{(k)}\right\}.$$

Furthermore the maximum efficiency is obtained for the incoming state which is equal to the eigenvector with the associated maximum eigenvalue $\max\{\lambda^{(k)}\} = \lambda^{(m)}$, meaning

$$\eta_s = \eta_s^{\max} \quad \text{for} \quad |\boldsymbol{\mathcal{E}}_{\text{in}}\rangle = \left|\boldsymbol{\mathcal{E}}_s^{(m)}\right\rangle \quad \text{and} \quad \eta_r = \eta_r^{\max} \quad \text{for} \quad |\mathbf{s}\rangle = \left|\mathbf{s}_r^{(m)}\right\rangle.$$

Because the matrices $\mathbf{M}^{\dagger}\mathbf{M}$ and $\mathbf{M}\mathbf{M}^{\dagger}$ have identical eigenvalues, we can conclude that the same maximum efficiency is obtained during storage and retrieval $\eta_s^{\max} = \eta_r^{\max}$ for $\mathbf{M} = \mathbf{M}'$. Moreover, we can deduce that we in this case store the light field into the optimal spin wave, which subsequently allows for retrieval with maximal efficiency.

$$\mathbf{M}\left|\boldsymbol{\mathcal{E}}_s^{(m)}\right\rangle \propto \left|\mathbf{s}_s^{(m)}\right\rangle = \left|\mathbf{s}_r^{(m)}\right\rangle \tag{5.5}$$

This means that the total retrieval is equal to $\eta_t = \eta_s^{\max}\eta_r^{\max}$ for $|\boldsymbol{\mathcal{E}}_{\text{in}}\rangle = |\boldsymbol{\mathcal{E}}_s^{(m)}\rangle$ and we therefore have maximized the whole process.

Now we have to determine what the condition $\mathbf{M} = \mathbf{M}'$ corresponds to and when it can be fulfilled. Using the formalism of the previous chapters, the linear maps between quantum field and spin wave can also be expressed as

$$\mathbf{s}(T) = \int_{-\infty}^{T} \mathbf{m}(\boldsymbol{\Delta}_s, T-t)\mathcal{E}_{\text{in}}(t)dt \tag{5.6}$$

$$\mathcal{E}_{\text{out}}(t) = \mathbf{m}'(\boldsymbol{\Delta}_r, t-T)^\dagger \mathbf{s}(T) \tag{5.7}$$

where we from the dynamics in Eq. (3.3) and Eq. (3.6) for constant Rabi oscillations find that

$$\mathbf{m}(\boldsymbol{\Delta}_s, T-t) = e^{-\mathbf{A}(T-t)}\mathbf{w} = -\sqrt{\frac{2}{\kappa}} \exp\left[-\boldsymbol{\Omega}^\dagger \boldsymbol{\Gamma}^{-1} \boldsymbol{\Omega}\,(T-t)\right] \boldsymbol{\Omega}^\dagger \boldsymbol{\Gamma}^{-1} \mathbf{g} \tag{5.8}$$

$$\mathbf{m}'(\boldsymbol{\Delta}_r, T-t) = e^{-\mathbf{A}^\dagger(T-t)}\mathbf{v} = -\sqrt{\frac{2}{\kappa}} \exp\left[-\boldsymbol{\Omega}^\dagger \left(\boldsymbol{\Gamma}^{-1}\right)^\dagger \boldsymbol{\Omega}\,(T-t)\right] \boldsymbol{\Omega}^\dagger \left(\boldsymbol{\Gamma}^{-1}\right)^\dagger \mathbf{g}. \tag{5.9}$$

The condition $\mathbf{M} = \mathbf{M}'$ in the Schrödinger picture corresponds in this formalism to requiring $\mathbf{m}(\boldsymbol{\Delta}_s, T-t) = \mathbf{m}'(\boldsymbol{\Delta}_r, T-t)$. This condition is in general not fulfilled, because $\boldsymbol{\Gamma}^{-1}$ is not hermitian. However, for systems without inhomogeneous broadening and uniform detuning $\boldsymbol{\Delta} = \Delta\mathbf{I}$ we know from Eq. (3.5) that

$$\boldsymbol{\Gamma}^{-1} = \tilde{\boldsymbol{\Delta}}^{-1} - \frac{\tilde{\boldsymbol{\Delta}}^{-1}\mathbf{g}\mathbf{g}^T\tilde{\boldsymbol{\Delta}}^{-1}}{\kappa + \mathbf{g}^T\tilde{\boldsymbol{\Delta}}^{-1}\mathbf{g}} = \frac{1}{\gamma + i\Delta}\left(\mathbf{I} - \frac{\mathbf{g}\mathbf{g}^T}{\kappa(\gamma + i\Delta) + \mathbf{g}^T\mathbf{g}}\right). \tag{5.10}$$

Now we see that in this case the condition $\mathbf{m}(\Delta_s, T-t) = \mathbf{m}'(\Delta_r, T-t)$ can be fulfilled when opposite detuning is used during storage and retrieval such that $\Delta_s = -\Delta_r$. This means that it is possible to maximize both the storage and the retrieval efficiency and that $\eta_t^{\max} = \eta_s^{\max}\eta_r^{\max}$.

This is however not possible when we account for inhomogeneous broadening. The condition $\mathbf{m}(\Delta_s, T-t) = \mathbf{m}'(\Delta_r, T-t)$ would be fulfilled for $\boldsymbol{\Delta}_s = -\boldsymbol{\Delta}_r$, but this cannot be realized physically. During storage we define $\boldsymbol{\Delta}_s = \Delta_s + \boldsymbol{\Delta}_{\text{atoms}}$ and during retrieval $\boldsymbol{\Delta}_r = \Delta_r + \boldsymbol{\Delta}_{\text{atoms}}$, where $\boldsymbol{\Delta}_{\text{atoms}}$ contains the inhomogeneities embedded into the ensemble and Δ_s, Δ_r denotes the uniform detunings which can be adjusted by using different light fields. Clearly, the condition $\boldsymbol{\Delta}_s = -\boldsymbol{\Delta}_r$ cannot be fulfilled by adjusting the uniform detunings Δ_s and Δ_r. This means that it is not sufficient for a medium with inhomogeneous broadening to optimize retrieval for itself and storage for itself, when we want to maximize the total efficiency. Furthermore we have to find a different argument which can be used to find the storage efficiency with the analysis of the retrieval process. It is here, where the time-reversal argument becomes very useful.

5.2 Time-reversal argument

The time-reversal argument allows us to find the optimal strategy for the storage process from retrieval. It has been proven in detail in [42] and we will here describe the essence of the argument. In order to illustrate the argument, we stay in the

Schrödinger picture for simplicity. During retrieval the transformation from the spin wave $|\mathbf{s}\rangle \in A$ to the outgoing light field $|\mathcal{E}_{\text{out}}\rangle \in B$ can be described with the unitary evolution operator $\hat{U}(T,0)$, where retrieval starts at $t = 0$ and ends at $t = T$. The retrieval efficiency is then given by $\eta_r = |\hat{P}_B \hat{U}(T,0)\,|\mathbf{s}\rangle\,|^2$, where $\hat{P}_B$ is the projection operator on the subspace B of the photon modes. Instead of the retrieval efficiency we are however going to make use of the overlap efficiency of a state $|a\rangle \in A$ with a state $|b\rangle \in B$.

$$\eta = |\langle b|\hat{U}(T,0)|a\rangle|^2 = |\langle a|\hat{U}^{-1}(T,0)|b\rangle|^2 \tag{5.11}$$

For the states $|a\rangle = |\mathbf{s}\rangle$ and $|b\rangle = |\boldsymbol{\mathcal{E}}_{\text{out}}\rangle$ this overlap efficiency is equal to the retrieval efficiency. Because the right hand side of the equation describes the overlap efficiency for the storage process, the storage efficiency is then equal to the retrieval efficiency. For this to be useful, we have to figure out how $\hat{U}^{-1}(T,0)$ can be realized physically. In Appendix C of [42] it has been shown that the inversion can be described with the time inversion operator $\hat{\tau}$ such that

$$\hat{U}^{-1}(T,0) = \hat{\tau}\hat{U}(T,0)\hat{\tau}. \tag{5.12}$$

Applying the time reverse operator to the spin wave state gives the complex conjugate such that $\tau\,|\mathbf{s}\rangle$ corresponds to $\mathbf{s}^*$, while applying it to the light field gives the time reverse such that $\hat{\tau}\,|\boldsymbol{\mathcal{E}}_{\text{out}}\rangle$ corresponds to $\mathcal{E}^*_{\text{out}}(T-t)$. This means that we can store $\mathcal{E}^*_{\text{out}}(T-t)$ into $\mathbf{s}^*$ with the storage overlap efficiency equal to the retrieval efficiency for $\mathbf{s}$ into $\mathcal{E}_{\text{out}}$.

If the maximal retrieval efficiency $\eta_r^{\max}$ is obtained for retrieving $\mathbf{s}^{\max}$ into $\mathcal{E}^{\max}_{\text{out}}(t)$, we know I. that it is not possible to achieve a higher storage efficiency than the maximal retrieval efficiency such that $\eta_s^{\max} = \eta_r^{\max}$. If it would be possible to get a higher storage efficiency $\eta_s > \eta_r^{\max}$ for storing some state $\mathcal{E}'_{\text{in}}$ into $\mathbf{s}'$, we could apply the time reversal argument and retrieve from $\mathbf{s}'$ with a higher retrieval efficiency than the maximal retrieval efficiency, which obviously is a contradiction. II. we have found that the maximal storage efficiency $\eta_s^{\max}$ is obtained for storage from $(\mathcal{E}^{\max}_{\text{out}}(T-t))^*$ into $(\mathbf{s}^{\max})^*$.

The fact that we can retrieve with $\eta_r^{\max}$ from $\mathbf{s}^{\max}$, but only store into $(\mathbf{s}^{\max})^*$ with $\eta_s^{\max}$ makes it more complicated to optimize the whole process of storage followed by retrieval. For real $\mathbf{s}^{\max}$ it is possible to obtain $\eta_t = \eta_s^{\max}\eta_r^{\max}$. However, for complex $\mathbf{s}^{\max}$ we have that $\eta_r[(\mathbf{s}^{\max})^*] < \eta_r^{\max}$ and it is therefore not possible to obtain the total efficiency $\eta_t = \eta_s^{\max}\eta_r^{\max}$. Furthermore we cannot conclude that storage into $\mathbf{s}^{\max}$ with subsequent retrieval from $\mathbf{s}^{\max}$ optimizes the total efficiency. If we denote the storage efficiency for storage into the spin wave $\mathbf{s}$ by $\eta_s(\mathbf{s})$ the total efficiency is given by

$$\eta_t(\mathbf{s}) = \eta_s(\mathbf{s})\eta_r(\mathbf{s}) = \eta_r(\mathbf{s}^*)\eta_r(\mathbf{s}) \tag{5.13}$$

where the time reversal argument has been used to write η_s in terms of η_r. The task is therefore to optimize $\eta_r(\mathbf{s}^*)\eta_r(\mathbf{s})$ with respect to $\mathbf{s}$ in order to find the maximal total efficiency.

5.3 Numerical solution for storage followed by retrieval

In this section we present a numerical method, which calculates the maximal total efficiency of storage followed by retrieval for a medium with any distribution of $\{g^{(i)}\}$, $\{\Omega^{(i)}\}$ and $\{\Delta^{(i)}\}$. When the input mode $\mathcal{E}_{\text{in}}(t)$ is normalized according to $\int_{-\infty}^{T_r} |\mathcal{E}_{\text{in}}(t)|^2 = 1$, the total efficiency of storage followed by retrieval is given by

$$\eta_{\text{tot}} = \frac{(\text{number of retrieved photons})}{(\text{number of incoming photons})} = \int_{T_r}^{\infty} dt |\mathcal{E}_{\text{out}}(t)|^2. \tag{5.14}$$

For time-independent Rabi oscillations in $\mathbf{\Omega}$ the dynamics of the spin wave during storage and the output mode during retrieval, which immediately follows the storage process, are through Eq. (3.3) and Eq. (3.6) given by:

$$\mathbf{s}(T_r) = \int_{-\infty}^{T_r} dt\, e^{-\mathbf{A}(T_r - t)} \mathbf{w} \mathcal{E}_{\text{in}}(t) \tag{5.15}$$

$$\mathcal{E}_{\text{out}}(t) = \mathbf{v}^\dagger e^{-\mathbf{A}(t-T_r)} \mathbf{s}(T_r) = \int_{-\infty}^{T_r} dt'\, \mathbf{v}^\dagger e^{-\mathbf{A}t} e^{\mathbf{A}t'} \mathbf{w} \mathcal{E}_{\text{in}}(t') \tag{5.16}$$

According to the fundamental dynamics of the quantum memory, the vector $\mathbf{w}$ is defined slightly different than $\mathbf{v} = -\sqrt{2/\kappa}\, \mathbf{\Omega}^\dagger \left(\mathbf{\Gamma}^{-1}\right)^\dagger \mathbf{g}$

$$\mathbf{w} = -\sqrt{\frac{2}{\kappa}} \mathbf{\Omega}^\dagger \mathbf{\Gamma}^{-1} \mathbf{g}. \tag{5.17}$$

This is similar to the definitions in Eq. (5.8) and Eq. (5.9). The total efficiency when setting $T_r = 0$ is then

$$\begin{aligned} \eta_{\text{tot}} &= \int_{-\infty}^{0} \int_{-\infty}^{0} \mathcal{E}_{\text{in}}^*(t'') \mathbf{w}^\dagger e^{\mathbf{A}^\dagger t''} \int_0^{\infty} e^{-\mathbf{A}^\dagger t} \mathbf{v}\mathbf{v}^\dagger e^{-\mathbf{A}t} dt\, e^{\mathbf{A}t'} \mathbf{w} \mathcal{E}_{\text{in}}(t') dt' dt'' \\ &= \int_{-\infty}^{0} \int_{-\infty}^{0} \mathcal{E}_{\text{in}}^*(t'') \mathbf{w}^\dagger e^{\mathbf{A}^\dagger t''} (-\mathbf{B})\, e^{\mathbf{A}t'} \mathbf{w} \mathcal{E}_{\text{in}}(t') dt' dt'' \end{aligned} \tag{5.18}$$

In order to calculate the integral over t, the same procedure as described in section 3.2 can be used, where $\mathbf{B}$ is determined using the Sylvester equation. The maximal total efficiency can be found by discretizing the time domain into N_t steps.

$$\begin{aligned} \eta_{\text{tot}} &= \sum_{t'=t_{\min}}^{t_{\max}} \sum_{t''=t_{\min}}^{t_{\max}} \mathcal{E}_{\text{in}}^*(t'') M(t', t'') \mathcal{E}_{\text{in}}(t') \left(\frac{t_{\max} - t_{\min}}{N_t} \right)^2 \\ &= \frac{\sum_{t'=t_{\min}}^{t_{\max}} \sum_{t''=t_{\min}}^{t_{\max}} \mathcal{E}_{\text{in}}^*(t'') M(t', t'') \frac{t_{\max} - t_{\min}}{N_t} \mathcal{E}_{\text{in}}(t')}{\sum_{t=t_{\min}}^{t_{\max}} |\mathcal{E}_{\text{in}}(t)|^2} \end{aligned} \tag{5.19}$$

Here we have defined the matrix elements in the discretized time domain as

$$M(t', t'') = -\mathbf{w}^\dagger e^{\mathbf{A}^\dagger t''} \mathbf{B} e^{\mathbf{A}t'} \mathbf{w}. \tag{5.20}$$

From this definition, the corresponding matrix $\mathbf{M}$ with a basis in the discretized time domain can be created. According to the variational principle the maximum total efficiency is the maximum eigenvalue of $\mathbf{M}$ multiplied by $(t_{\max} - t_{\min})/N_t$.

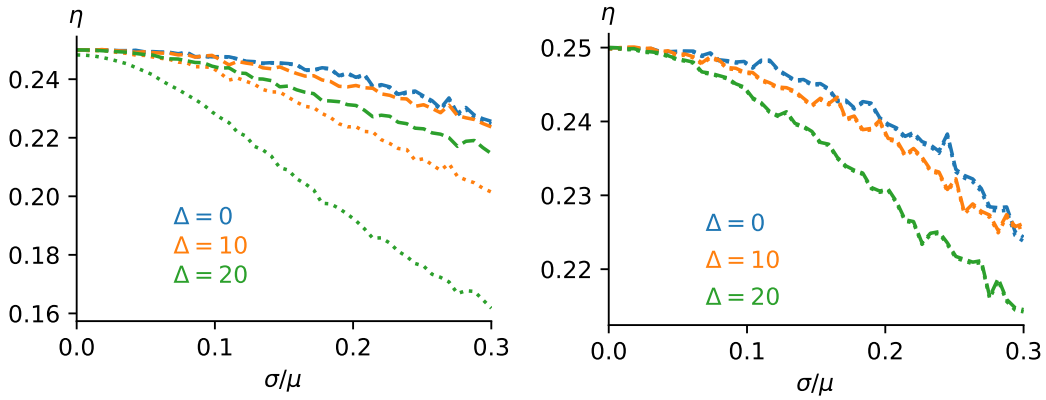

(a) (b)

Figure 5.1: Maximal total efficiency $\eta_t^{\max}$ (dotted lines) and maximal retrieval efficiency squared $(\eta_r^{\max})^2$ (dashed lines) as a function of $\sigma/\mu = \sigma_\Omega/\mu_\Omega = \sigma_g/\mu_g$ for different detuning. The dashed and dotted lines overlap in (b). In order to smooth out variation in the numerical solutions, the data points of the numerical solution are averages of 20 calculations with $N = 150$ random samples drawn from a Gaussian distribution. The following values have been used in the calculations: $\gamma = 10$, $\kappa = 15$, $g = 1$, $\Omega = 10$. In (a) the same detuning is used during storage and retrieval and in (b) the detuning is inverted after storage.

5.4 Inhomogenous Rabi oscillations $\Omega^{(i)}$ and coupling constant $g^{(i)}$

In this section, we will look at the maximal total efficiency for media, which has inhomogeneities with Gaussian distributions of $\{\Omega^{(i)}\}$ and $\{g^{(i)}\}$, but is homogeneously broadened. Furthermore we will examine how the maximal total efficiency is related to the maximal retrieval efficiency, which has been analyzed in the previous chapter. We limit our calculations to the case where the Λ energy scheme only consists of one excited state.

In Figure 5.1 we have calculated the maximal total efficiency numerically and compared it with the numerical solution for the maximal retrieval efficiency. First, in (a), we have looked at the case where detuning remains unchanged during storage and retrieval $\Delta_s = \Delta_r$. For $\Delta = 0$ the maximal total efficiency is equal to the square of the maximal retrieval efficiency $\eta_t = \eta_r^2$. With increasing detuning the solutions for $\eta_t^{\max}$ and $(\eta_r^{\max})^2$ do however deviate more and more from each other for specific $\sigma/\mu = \sigma_\Omega/\mu_\Omega = \sigma_g/\mu_g$ with $\eta_t^{\max}$ having lower efficiencies. Furthermore the deviations increase at a specific nonzero detuning Δ with increasing standard deviations. In (b) the solutions for $\eta_t^{\max}$ and $(\eta_r^{\max})^2$ overlap. This is also what we would have expected from the analysis in section 5.1.

The result in (a) for $\Delta_s = \Delta_r$ that maximal total retrieval equals to $\eta_t = \eta_r^2$ for zero detuning, but not for nonzero detuning, is also consistent with the time reversal argument, when we analyze the optimal spin wave which allows for retrieval with $\eta_r^{\max}$. According to Eq. (4.57) the spin wave is real for zero detuning, but complex

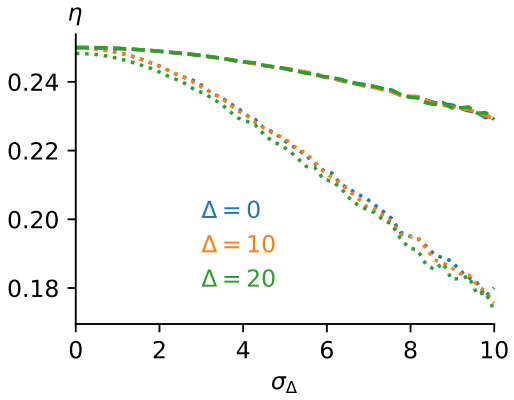

Figure 5.2: Maximal total efficiency $\eta_t^{\max}$ (dotted lines) and maximal retrieval efficiency squared $(\eta_r^{\max})^2$ (dashed lines) as a function of σ_Δ for different mean detuning. In order to smooth out variation in the numerical solutions, the data points of the numerical solution are averages of 100 calculations with $N = 150$ random samples drawn from a Gaussian distribution. The following values have been used in the calculations: $\rho = 0$, $\gamma = 10$, $\kappa = 15$, $\mu_g = 1$, $\mu_\Omega = 10$.

for nonzero detuning. From time reversal we know that the total efficiency is $\eta_t(\mathbf{s}) = \eta_r(\mathbf{s}^*)\eta_r(\mathbf{s})$. Since η_r is not invariant under complex conjugation of the spin wave, we would expect deviations of $\eta_t(\mathbf{s})$ from $\eta_r(\mathbf{s})^2$ for nonzero detuning.

The optimal strategy for storage followed by retrieval is therefore to be on-resonance. When this is not possible, the detunings should be inverted after storage.

5.5 Inhomogeneous broadening

We will now look at the maximum total efficiency for inhomogeneous broadened media with a Gaussian distribution of $\{\Delta^{(i)}\}$, but homogeneous Rabi oscillations $\{\Omega^{(i)}\}$ and coupling constant $\{g^{(i)}\}$. Again we restrict the model to the case where the Λ energy scheme only has one excited level.

The numerical results for $\eta_t^{\max}$ have been compared with the numerical results for $(\eta_r^{\max})^2$ in Figure 5.2 for equal detuning during storage and retrieval $\Delta_s = \Delta_r$. In contrast to medium without inhomogeneous broadening, the two different efficiencies also deviate for zero detuning μ_Δ. This means that there also is no overlap between $\eta_t^{\max}$ and $(\eta_r^{\max})^2$ for $\Delta_s = -\Delta_r$. Furthermore, the results suggest that both efficiencies are completely independent of the average detuning. Again the deviations between $\eta_t^{\max}$ and $(\eta_r^{\max})^2$ increase with increasing standard deviation. With respect to the time-reversal argument, these results suggest that the initial spin wave is complex.

We can conclude that the optimal strategy for storage followed by retrieval is independent of the average detuning for systems with inhomogeneous broadening.

Chapter 6

Conclusion and outlook

6.1 Conclusion

In this thesis, we have investigated how inhomogeneities affect the efficiency of Λ-type quantum memories within a cavity. For systems with inhomogeneities in the coupling constants, but homogeneous Rabi oscillations and without inhomogeneous broadening, we found that the retrieval efficiency does not decrease. In this case only a single spin wave mode is accessible and can be coupled to the incoming and outgoing light fields. On the other hand, for inhomogeneous Rabi oscillations and otherwise homogeneous parameters, we found that the retrieval efficiency did decrease. This has been observed through numerical calculations for random samples from several different continuous distributions. Not all distributions did however have the same efficiency dependence on the distribution width. While the dependence for Gaussian and Uniform distributions was second order, it was qualitatively different for Lorentzian distributions.

Subsequently, we focused on developing a symbolic method for calculating the retrieval efficiency perturbatively, which also can be applied to systems with inhomogeneous Rabi oscillations and inhomogeneous broadening and is valid for population distributions with well-defined moments. In contrast to memories with inhomogeneities only in the coupling constant, several spin wave modes become accessible, making the derivation more complicated. By comparison with numerical calculations, we found that the method is accurate to second order for Gaussian inhomogeneities. While the maximal retrieval efficiency was independent of the applied detuning for inhomogeneously broadened media, a higher maximal retrieval efficiency was derived for on-resonant quantum memories with inhomogeneous Rabi oscillations and coupling constants.

In order to find the optimal strategy for storage followed by retrieval, the quantum field has to be coupled to a spin wave mode, which allows for both efficient storage and retrieval. When the applied detuning is reversed after storage, the same spin wave mode, which allows for optimal storage, allows also for optimal retrieval. This is however not true for inhomogeneously broadened media, leading to a smaller maximal storage-retrieval efficiency when compared with the squared maximal retrieval efficiency. Moreover, just as the maximal retrieval efficiency was independent of ap-

plied detuning, the same was true for the maximal storage-retrieval efficiency. The optimal strategy is therefore independent of applied detuning for quantum memories with inhomogeneous broadening. For systems with inhomogeneous Rabi oscillations and coupling constant the optimal strategy is to apply on-resonant optical fields.

6.2 Outlook

This thesis provides the basis for several topics, which could be investigated further. The maximal storage-retrieval efficiency has only been calculated numerically and it would therefore be useful to develop the symbolic method further such that it also can be used to analyze the full process. Because the symbolic method in this thesis only can be applied directly to the retrieval efficiency, the time-reversal argument could be a very useful tool to expand the method. The formalism for deriving $\eta_r(\mathbf{s})$ already exist. It would therefore only have to be applied for $\eta_r(\mathbf{s}^*)\eta_r(\mathbf{s})$ and optimized with respect to $\mathbf{s}$. First order terms that vanish in $\langle\eta_r(\mathbf{s})\rangle$ might however become second order in $\langle\eta_r(\mathbf{s}^*)\eta_r(\mathbf{s})\rangle$, so one has to make sure to derive a formula for $\langle\eta_r(\mathbf{s}^*)\eta_r(\mathbf{s})\rangle$ and not $\langle\eta_r(\mathbf{s}^*)\rangle\langle\eta_r(\mathbf{s})\rangle$.

Secondly, quantum memories with inhomogeneous broadening and inhomogeneities in Rabi oscillations and coupling constants could be analyzed including the effect of correlations between the different inhomogeneities. Both the numerical and the symbolic methods developed in this thesis can directly be applied to this problem. Lastly, specific physical systems, such as NV-centers with several excited states, could be considered.

Bibliography

[1] Lene Vestergaard Hau, S. E. Harris, Zachary Dutton, and Cyrus H. Behroozi. Light speed reduction to 17 metres per second in an ultracold atomic gas. *Nature*, 397:594, Feb 1999.

[2] Morgan P. Hedges, Jevon J. Longdell, Yongmin Li, and Matthew J. Sellars. Efficient quantum memory for light. *Nature*, 465:1052, Jun 2010.

[3] Pierre Vernaz-Gris, Kun Huang, Mingtao Cao, Alexandra S. Sheremet, and Julien Laurat. Highly-efficient quantum memory for polarization qubits in a spatially-multiplexed cold atomic ensemble. *Nature Communications*, 9(1):363, 2018.

[4] Alexey V. Gorshkov, Axel André, Mikhail D. Lukin, and Anders S. Sørensen. Photon storage in Λ-type optically dense atomic media. iii. effects of inhomogeneous broadening. *Phys. Rev. A*, 76:033806, Sep 2007.

[5] Klemens Hammerer, Anders S. Sørensen, and Eugene S. Polzik. Quantum interface between light and atomic ensembles. *Rev. Mod. Phys.*, 82:1041–1093, Apr 2010.

[6] Khabat Heshami, Duncan G. England, Peter C. Humphreys, Philip J. Bustard, Victor M. Acosta, Joshua Nunn, and Benjamin J. Sussman. Quantum memories: emerging applications and recent advances. *Journal of Modern Optics*, 63(20):2005–2028, 2016.

[7] Alexander I. Lvovsky, Barry C. Sanders, and Wolfgang Tittel. Optical quantum memory. *Nature Photonics*, 3:706, Dec 2009. Review Article.

[8] M. Fleischhauer and M. D. Lukin. Dark-state polaritons in electromagnetically induced transparency. *Phys. Rev. Lett.*, 84:5094–5097, May 2000.

[9] Alexey V. Gorshkov, Axel André, Mikhail D. Lukin, and Anders S. Sørensen. Photon storage in Λ-type optically dense atomic media. i. cavity model. *Phys. Rev. A*, 76:033804, Sep 2007.

[10] K.-J. Boller, A. Imamoğlu, and S. E. Harris. Observation of electromagnetically induced transparency. *Phys. Rev. Lett.*, 66:2593–2596, May 1991.

[11] M. D. Lukin. Colloquium. *Rev. Mod. Phys.*, 75:457–472, Apr 2003.

[12] Michael Fleischhauer, Atac Imamoglu, and Jonathan P. Marangos. Electromagnetically induced transparency: Optics in coherent media. *Rev. Mod. Phys.*, 77:633–673, Jul 2005.

[13] M. Fleischhauer and M. D. Lukin. Quantum memory for photons: Dark-state polaritons. *Phys. Rev. A*, 65:022314, Jan 2002.

[14] A. E. Kozhekin, K. Mølmer, and E. Polzik. Quantum memory for light. *Phys. Rev. A*, 62:033809, Aug 2000.

[15] O. S. Mishina, D. V. Kupriyanov, J. H. Müller, and E. S. Polzik. Spectral theory of quantum memory and entanglement via raman scattering of light by an atomic ensemble. *Phys. Rev. A*, 75:042326, Apr 2007.

[16] J. Nunn, I. A. Walmsley, M. G. Raymer, K. Surmacz, F. C. Waldermann, Z. Wang, and D. Jaksch. Mapping broadband single-photon wave packets into an atomic memory. *Phys. Rev. A*, 75:011401, Jan 2007.

[17] Mikael Afzelius, Christoph Simon, Hugues de Riedmatten, and Nicolas Gisin. Multimode quantum memory based on atomic frequency combs. *Phys. Rev. A*, 79:052329, May 2009.

[18] B. Kraus, W. Tittel, N. Gisin, M. Nilsson, S. Kröll, and J. I. Cirac. Quantum memory for nonstationary light fields based on controlled reversible inhomogeneous broadening. *Phys. Rev. A*, 73:020302, Feb 2006.

[19] D. F. Phillips, A. Fleischhauer, A. Mair, R. L. Walsworth, and M. D. Lukin. Storage of light in atomic vapor. *Phys. Rev. Lett.*, 86:783–786, Jan 2001.

[20] Chien Liu, Zachary Dutton, Cyrus H. Behroozi, and Lene Vestergaard Hau. Observation of coherent optical information storage in an atomic medium using halted light pulses. *Nature*, 409:490, Jan 2001.

[21] Brian Julsgaard, Jacob Sherson, J. Ignacio Cirac, Jaromír Fiurásek, and Eugene S. Polzik. Experimental demonstration of quantum memory for light. *Nature*, 432:482, Nov 2004.

[22] Y. O. Dudin, L. Li, and A. Kuzmich. Light storage on the time scale of a minute. *Phys. Rev. A*, 87:031801, Mar 2013.

[23] Georg Heinze, Christian Hubrich, and Thomas Halfmann. Stopped light and image storage by electromagnetically induced transparency up to the regime of one minute. *Phys. Rev. Lett.*, 111:033601, Jul 2013.

[24] Manjin Zhong, Morgan P. Hedges, Rose L. Ahlefeldt, John G. Bartholomew, Sarah E. Beavan, Sven M. Wittig, Jevon J. Longdell, and Matthew J. Sellars. Optically addressable nuclear spins in a solid with a six-hour coherence time. *Nature*, 517:177, Jan 2015.

[25] J. Nunn, K. Reim, K. C. Lee, V. O. Lorenz, B. J. Sussman, I. A. Walmsley, and D. Jaksch. Multimode memories in atomic ensembles. *Phys. Rev. Lett.*, 101:260502, Dec 2008.

[26] Mahmood Sabooni, Qian Li, Stefan Kröll, and Lars Rippe. Efficient quantum memory using a weakly absorbing sample. *Phys. Rev. Lett.*, 110:133604, Mar 2013.

[27] V. M. Acosta, K. Jensen, C. Santori, D. Budker, and R. G. Beausoleil. Electromagnetically induced transparency in a diamond spin ensemble enables all-optical electromagnetic field sensing. *Phys. Rev. Lett.*, 110:213605, May 2013.

[28] Philip J. Bustard, Rune Lausten, Duncan G. England, and Benjamin J. Sussman. Toward quantum processing in molecules: A thz-bandwidth coherent memory for light. *Phys. Rev. Lett.*, 111:083901, Aug 2013.

[29] Duncan G. England, Kent A. G. Fisher, Jean-Philippe W. MacLean, Philip J. Bustard, Rune Lausten, Kevin J. Resch, and Benjamin J. Sussman. Storage and retrieval of thz-bandwidth single photons using a room-temperature diamond quantum memory. *Phys. Rev. Lett.*, 114:053602, Feb 2015.

[30] L.-M. Duan, M. D. Lukin, J. I. Cirac, and P. Zoller. Long-distance quantum communication with atomic ensembles and linear optics. *Nature*, 414:413, Nov 2001. Article.

[31] Christoph Simon, Hugues de Riedmatten, Mikael Afzelius, Nicolas Sangouard, Hugo Zbinden, and Nicolas Gisin. Quantum repeaters with photon pair sources and multimode memories. *Phys. Rev. Lett.*, 98:190503, May 2007.

[32] Nicolas Sangouard, Christoph Simon, Bo Zhao, Yu-Ao Chen, Hugues de Riedmatten, Jian-Wei Pan, and Nicolas Gisin. Robust and efficient quantum repeaters with atomic ensembles and linear optics. *Phys. Rev. A*, 77:062301, Jun 2008.

[33] Félix Bussières, Nicolas Sangouard, Mikael Afzelius, Hugues de Riedmatten, Christoph Simon, and Wolfgang Tittel. Prospective applications of optical quantum memories. *Journal of Modern Optics*, 60(18):1519–1537, 2013.

[34] D. F. Walls and G. J. Milburn. *Quantum Optics*, chapter 7, pages 127–131. Springer Verlag Berlin Heidelberg, 2008.

[35] Nathaniel B. Phillips, Alexey V. Gorshkov, and Irina Novikova. Optimal light storage in atomic vapor. *Phys. Rev. A*, 78:023801, Aug 2008.

[36] Marlis Hochbruck and Christian Lubich. On krylov subspace approximations to the matrix exponential operator. *SIAM Journal on Numerical Analysis*, 34(5):1911–1925, 1997.

[37] Mikhail A. Bochev. *A short guide to exponential Krylov subspace time integration for Maxwell's equations.* Number 1992 in Memorandum. Department of Applied Mathematics, University of Twente, 9 2012.

[38] J. F. Kenney and E. S. Keeping. *Mathematics of Statistics*, chapter 7, page 164. 2. D. Van Nostrand Company, 2 edition, 1951.

[39] Xiaobo Zhu, Shiro Saito, Alexander Kemp, Kosuke Kakuyanagi, Shin-ichi Karimoto, Hayato Nakano, William J. Munro, Yasuhiro Tokura, Mark S. Everitt, Kae Nemoto, Makoto Kasu, Norikazu Mizuochi, and Kouichi Semba. Coherent coupling of a superconducting flux qubit to an electron spin ensemble in diamond. *Nature*, 478:221, Oct 2011.

[40] Hua Wu, Richard E. George, Janus H. Wesenberg, Klaus Mølmer, David I. Schuster, Robert J. Schoelkopf, Kohei M. Itoh, Arzhang Ardavan, John J. L. Morton, and G. Andrew D. Briggs. Storage of multiple coherent microwave excitations in an electron spin ensemble. *Phys. Rev. Lett.*, 105:140503, Sep 2010.

[41] Khabat Heshami, Charles Santori, Behzad Khanaliloo, Chris Healey, Victor M. Acosta, Paul E. Barclay, and Christoph Simon. Raman quantum memory based on an ensemble of nitrogen-vacancy centers coupled to a microcavity. *Phys. Rev. A*, 89:040301, Apr 2014.

[42] Alexey V. Gorshkov, Axel André, Mikhail D. Lukin, and Anders S. Sørensen. Photon storage in Λ-type optically dense atomic media. ii. free-space model. *Phys. Rev. A*, 76:033805, Sep 2007.